

Effect of Working Fluid on Thermodynamic Performance Analysis of Organic Rankine Cycle (ORC)

*A Dissertation submitted to the
Delhi Technological University
in partial fulfillment of the requirements
of the award of the degree of
Masters of Technology
(Thermal Engineering)*

By

Sitansu Satyapriya Rout

Roll No. 2K20/THE/18

under the supervision of

Prof. B.B Arora

Mechanical Engineering Department



*Delhi Technological University
(Formerly Delhi College of Engineering)
Shahbad Daultapur, Bawana Road Delhi-110042*

DECLARATION OF ORIGINALITY

I hereby declare that this submission is my own work and that, to the best of my knowledge and belief, it contains neither materials previously published or written by another person nor any materials presented for the award of any degree or diploma of Delhi Technological University or any other institution of higher learning. Any contribution made to this research by others is explicitly acknowledged in the dissertation.

Student's Signature

CERTIFICATE

This is to certify that the work presented in this dissertation “*Effect of Working Fluids on Thermodynamic Performance Analysis of Organic Rankine Cycle (ORC)*” by Sitansu Satyapriya Rout, Roll No. 2K20/THE/18, is a record of original research carried out by him under my supervision and guidance in partial fulfilment of the requirements for the degree of *Master of Technology (Thermal Engineering)*. Neither this dissertation nor any part of it has been submitted earlier for any degree or diploma to any institute or university in India or abroad.

Supervisor's Signature

ACKNOWLEDGEMENTS

Foremost, I would like to express my heartfelt gratitude to Prof. B.B Arora, my research supervisor, for his patience, continuous support, encouragement, timely guidance, discussions and suggestions. His guidance, great moral support, and inspiration helped me throughout the journey of my research and the improvement of writing the thesis.

Besides my supervisor, I would like to thank Dr. S.K Garg, Professor (HOD) at Department of Mechanical Engineering, Delhi Technological University for his insightful comments, encouragement and valuable suggestions regarding the research work. Also, special thanks to the Mechanical Engineering Department of Delhi Technological University for the different facilities they offered.

For any errors or inadequacies that may remain in this work, of course, the responsibility is entirely my own.

Sitansu Satyapriya Rout
(2K20/THE/18)

ABSTRACT

Working fluids play a crucial part in Organic Rankine Cycle (ORC) which is able to recover the low-grade heat from renewable or waste heat sources. Current work focuses on establishing the relationship between ORC performance parameters (First law efficiency, Second law efficiency, Turbine Size Factor (TSF), net work output) and the source temperature, Turbine inlet Temperature Pinch point Temperature Difference and turbine efficiency by employing 4 different working fluid (RC318, R600a, R32, R134a).

The working fluids are so chosen that two are dry fluids (RC318, R600a) having higher critical temperature and two are wet fluids (R143a, R32) with comparatively lower critical temperature.

An EES program has been developed to analyse these performance parameters with varied input conditions.

The cycle efficiency increase monotonically with rising HST, TIT and turbine efficiency. On contrary TSF decreases with increasing HST, TIT and turbine efficiency. Net Work Output increases with increasing HST, TIT and Turbine Efficiency but decreases with increasing PPTD.

Keywords: *ORC, RC, First law efficiency, Second law efficiency, TSF, Net Work output, HST.*

CONTENTS

	Page No.
DECLARATION	i
SUPERVISOR'S CERTIFICATE	ii
ACKNOWLEDGEMENTS	iii
ABSTRACT.....	iv
CONTENTS	v
LIST OF FIGURES	vii
LIST OF TABLE	viii
CHAPTER-1 INTRODUCTION	1-12
1.1 General	1
1.2 History	2
1.3 Worldwide ORC Installation	3
1.4 Low Grade Temperature Heat Recovery Cycles	3
1.4.1 The Kalina Cycle	
1.4.2 Goswami Cycle	4
1.4.3 Trilateral Flash Cycle	5
1.4.4 Organic Rankine Cycle	6
1.5 Applications of ORC	6
1.5.1 Waste Heat Recovery	6
1.5.2 Solar Thermal Power	6
1.5.3 Geothermal Power Plants	7
1.5.4 Biomass Power Plant	8
1.6 ORC Market Share for Different Heat Source	8
1.7 The ORC and the Conventional Rankine Cycle	9
1.8 Working Fluid Selection	10
1.9 Thermodynamic Properties	10

1.10 Safety and Environmental Criteria	12
CHAPTER 2: LITERATURE REVIEW	13-18
2.1 Introduction	13
2.2 Organic Rankine Cycle Based Hybrid Systems	13
2.3 Waste Heat/Thermal Energy Powered ORC Based Hybrid Systems	14
2.4 Solar-Thermal Energy Powered ORC Based Hybrid Systems	15
2.5 Biomass Energy Powered ORC Based Hybrid Systems	16
2.6 Geothermal Energy Powered ORC Based Hybrid Systems	17
2.7 Micro Scale Organic Rankine Cycle	17
2.8 Present Work	18
2.9 Objectives of Study	18
CHAPTER 3 SYSTEM MODELING	19-21
3.1 System Modeling	19
3.2 System Description	19
3.2.1 Working Principle and Mathematical Models of SRC and ORC	21
3.3 Assumptions and Limits	20
3.4 The Set of Calculation Conditions	20
CHAPTER 4 RESULTS AND DISCUSSION	22-43
4.1 Effect of Heat Source Temperature	22
4.2 Effect of Turbine Inlet Temperature	28
4.3 Effect of Pinch Point Temperature Difference	32
4.4 Effect of Turbine Efficiency	38
CHAPTER 5 CONCLUSIONS AND FUTURE SCOPE	44-46
5.1 Conclusions	45
5.2 Future Scope	46
REFERENCES	46-50

LIST OF TABLE

Title	P.No
Table 4.1: Simulations results using R32	22
Table 4.2: Simulations results using R600a	23
Table 4.3: Simulations results using R134a	24
Table 4.4: Simulations results using RC318	24
Table 4.5: Simulation results after variation in turbine inlet temperatures using R32	28
Table 4.6: Simulation results after variation in turbine inlet temperatures using R600a	29
Table 4.7: Simulation results after variation in turbine inlet temperatures using R134a	29
Table 4.8: Simulation results after variation in turbine inlet temperatures using RC318	30
Table 4.9: Simulation results after variation in pinch point temperature difference using R32	33
Table 4.10: Simulation results after variation in pinch point temperature difference using R600a	33
Table 4.11: Simulation results after variation in pinch point temperature difference using R134a	34
Table 4.12: Simulation results after variation in pinch point temperature difference using RC318	35
Table 4.13: Simulation results after variation in turbine efficiency using R32	38
Table 4.14: Simulation results after variation in turbine efficiency using R600a	39
Table 4.15: Simulation results after variation in turbine efficiency using R134a	39
Table 4.16: Simulation results after variation in turbine efficiency using RC318	40

LIST OF FIGURE

Title	Page No.
Fig. 1.1: An article on naphtha engine	2
Fig. 1.2: Sample design of naphtha engine	3
Fig. 1.3: Kalina Cycle	4
Fig. 1.4: Goswami cycle	5
Fig. 1.5: Trilateral flash cycle	5
Fig. 1.6: ORC in waste heat recovery	6
Fig. 1.7: Solar thermal power plant	7
Fig. 1.8: Geothermal electric generation system	7
Fig. 1.9: Biomass ORC	8
Fig. 1.10: The ORC market share for different heat sources	9
Fig. 1.11: Isentropic working fluid T-s diagram	11
Fig. 1.12: Wet working fluid T-s diagram	11
Fig. 1.13: Dry working fluid T-s diagram	12
Fig. 3.1: Schematic diagram of the organic Rankine cycle	19
Fig. 4.1: I st Law efficiency vs. HST	25
Fig. 4.2: II nd Law Efficiency vs. HST	26
Fig. 4.3: TSF vs. HST	26
Fig. 4.4: Net Work Output vs. HST	27
Fig. 4.5: I st Law Efficiency vs. TSF	30
Fig. 4.6: II nd Law Efficiency vs. TIT	31
Fig. 4.7: TSF vs. TIT	31
Fig. 4.8: Net Work Output vs. TIT	32
Fig. 4.9: I st Law Efficiency vs. PPTD	35
Fig. 4.10: II nd Law Efficiency vs. PPTD	36
Fig. 4.11: TSF vs. PPTD	37
Fig. 4.12: Net Work Output vs. PPTD	37
Fig. 4.13: I st Law Efficiency vs. TE	40

Fig. 4.14: II nd Law Efficiency vs. TE	41
Fig. 4.15: TSF vs. TE	42
Fig. 4.16: Net Work Output vs. turbine efficiency	42

1.1 GENERAL INFORMATION

The world's current development is largely due to progressively effective and widespread usage of numerous practices of energy. Surge in global energy consumption in the last few decades has showed that fossil fuel vitality sources only will not be able to meet forthcoming energy demands.

The usage of IHE improves the first law efficiency. The exergetic efficiency for R1233zd[E] is higher than other fluids in comparison with R245fa and Novec 649[1]. Energy taking out from superheated steam, turbine exhaust, solar energy, as well as biomass energy becomes a typical method for most industry to generate alternative energy. Low-grade heat inputs can be turned into electrical energy by means of an ORC (Organic Rankine Cycle) system. The inherent concept of ORC is pretty similar with that of the Rankine cycle. The WF of ORC is having high vapor pressure and lower boiling point than water. When compared with conventional Rankine cycle, these features of organic fluids significantly improve ORC cycle efficiency. ORCs have been successfully installed in a number of locations throughout the world, and much more research is ongoing to improve the system.

Apart from of negative environmentally friendly consequences, fossil fuel rates are volatile, with utmost of time going up. Several countries are currently investing money in novel and effective energy skills as a substitute on behalf of fossil fuels in power generation. Low-quality heat can be found in a variety of places, including renewable energy sources or industrialized waste. Using present form of sustainable energy may possibly help minimize consumption of non-renewable energy, lowering non-renewable energy's environmental impact.

Effective and efficient solutions should be developed to get useful work from heat resources which are low grade heat resources. An ORC is an appropriate tool for accomplishing this goal. The ORC employs an organic WF with a large molecular mass and phase change of fluid to vapor that occurs on lower temperature than phase change of liquid to steam at the same pressure. Organic fluids can be used to recover heat from low-grade sources [2].

Industrial waste, Solar energy, Biomass energy, Geothermal energy are the prime members in low grade heat sources category. The ORC turns low-grade heat into work, which is then converted into electricity.

1.2 HISTROY

The focus in restoring low-grade heat has increased rapidly in recent years. Many researches have proposed a number of methods for producing electricity commencing lower-temperature heat source such as sun power, residential boiler, biomass, as well as industrialized waste heat. Due to the simpler construction, the ORC is seen to be the most suited of all. In 1883, Frank W. Ofledt patented naphtha engine, which serves similar purpose as ORC. To replace steam engine on the boat, naphtha was utilized as the WF replacing water. Liquid hydrocarbon naphtha is obtained through distillation process of crude petroleum oil. Because naphtha has a lower heat of vaporization than water, the situation was observed that if specific quantity of heat is supplied to naphtha, that one creates additional vapor besides hence higher work output from the engine if water is supplied. When steamboats started using naphtha engines, there was a large chance of explosion, and thus it was made obligatory for operators to obtain permits, which led to the naphtha engine's population increase [3]. Frank W.Ofledt's innovation was a viable alternative to steam engines. Figure 2.1 depicts a naphtha engine article from 1890, whereas figure 2.2 depicts a basic naphtha engine concept.

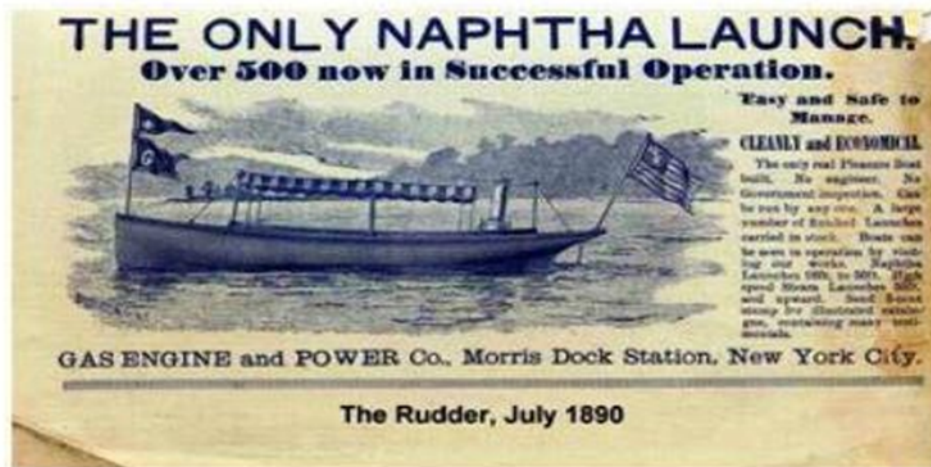


Figure 1.1 A naphtha engine article [3]

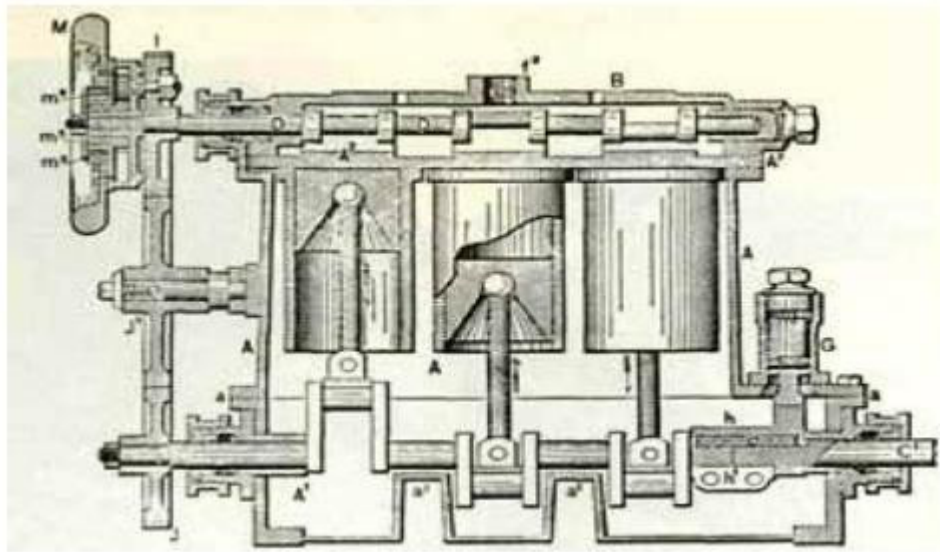


Figure 1.2 An example of a naphtha engine design [4]

Harry Zvi designed the very first model of the ORC development in timely 1960s. Present model was primarily secondhand to improve lower-grade heat, like to how sun power is recycled to convert low-temperature sources to electricity. Harry Zvi also invented a turbine that could work and operate at a relatively low temperature. An Israeli corporation later privatized this innovation in 1965 [5].

1.3 WORLDWIDE ORC INSTALLATION

ORC installations are currently successful in a number of nations. Various countries nowadays are utilizing waste heat with ORCs. The majority of ORC systems are found in Germany, Italy, Canada, and the United States, while Belgium, Austria, Romania, Russia, Finland, Swaziland, Morocco, and India have only one unit. Tas Energy, Ormat, and Turboden are the leading suppliers of ORC equipment. The gas, glass, and cement industries are the most common businesses that employ the ORC system for recovering waste heat in various nations [6].

1.4 LOW GRADE TEMPERATURE HEAT RECOVERY CYCLES

Using traditional Rankine cycles (RC) to alter thermal power as of a lower-grade heat sources to electricity is not cost-effective, particularly when temperature is exceedingly lower. Multiple cycles have already been designed to properly utilize energy from low-grade heat sources. Because organic WFs are employed instead of water, some of the invented cycles, such as the

Goswami cycle and ORC, provide larger profits or lower component prices. In the subsequent sections, the Kalina cycle, and Organic Rankine cycle are fleetingly explained.

1.4.1 KALINA CYCLE

It was designed to alter lower-grade heat into electrical energy. In the 1970s, Aleksander Kalina invented the first cycle. Water and ammonia were employed as working fluids to increase cycle efficiency while decreasing irreversibility. The Kalina cycle makes use of two thermally matched fluids. Studies on this cycle have shown that it outperforms the traditional Rankine cycle by a significant margin. The Kalina cycle is understood in Figure 1.3

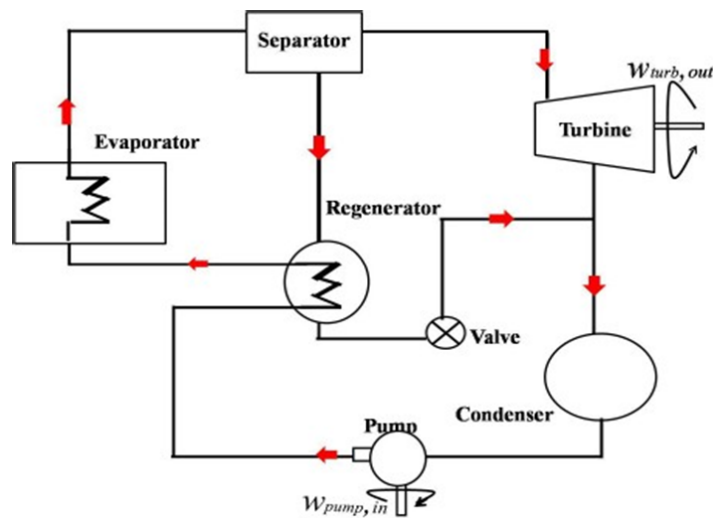


Fig. 1.3 Schematic of Kalina Cycle

1.4.2 TRILATERAL FLASH CYCLE

According to certain scientific articles, this cycle has more power than the flash steam system and perhaps the ORC method when it comes to recovering waste heat. The difficulty in finding proper expanders which is able to manage larger adiabatic efficiency as well as two-phase flow is a key drawback for this system. The trilateral flash cycle is shown in Figure 1.5.

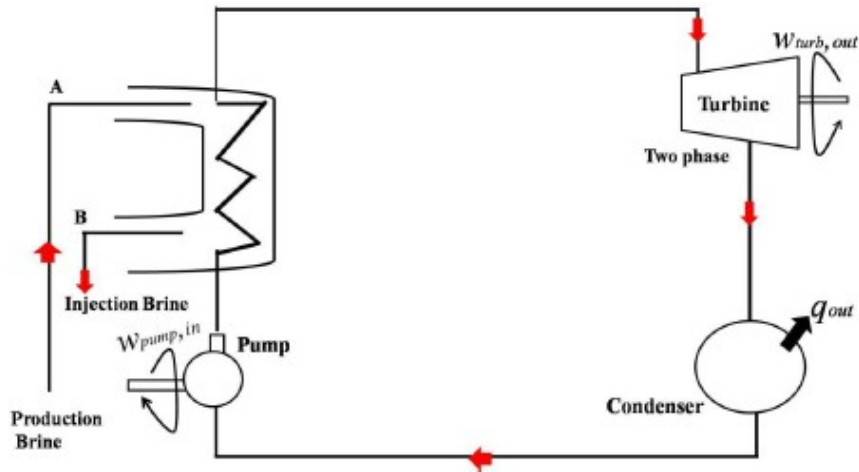


Figure 1.4 Representation of Trilateral flash cycle

1.4.3 GOSWAMI CYCLE

Dr. Yogi Goswami described the Goswami cycle for the first time in 1998 [6]. This novel thermodynamic cycle generates power with refrigeration in single loop using a binary mixture. The binary solution of NH_3 and H_2O boosts the cycle's energy resource usage. The system is capable of converting low-grade HSs into electrical energy and is also capable of providing combination of electric energy and refrigeration. It implies, the amount of electricity generated can be raised while cooling is reduced. The Goswami cycle is depicted below.

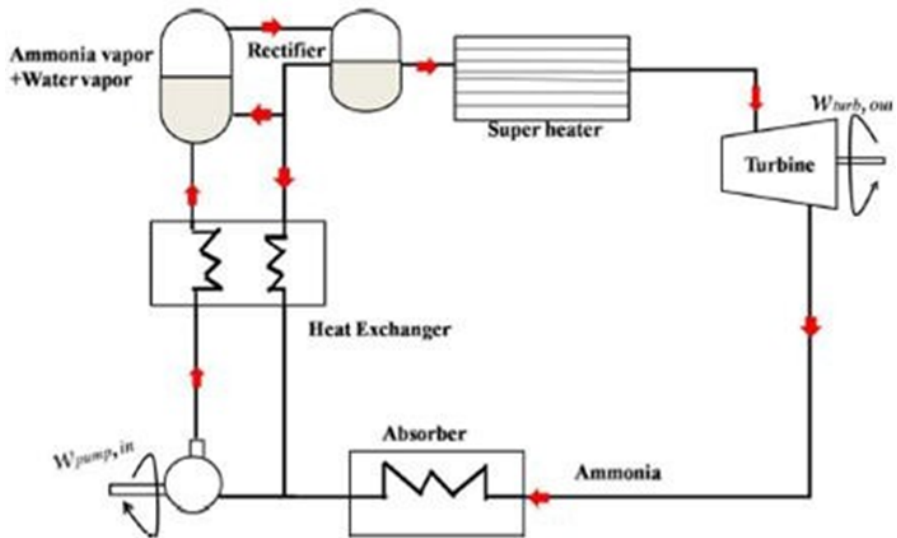


Figure 1.5 Representation of Goswami Cycle

1.4.4 ORGANIC RANKINE CYCLE (ORC)

ORC as well as standard RC both work on similar principles, as explained previously. The condenser, pump, evaporator (boiler), and expander are all identical components. Though there is a distinction in the types of working fluid employed in cycles. In comparison to traditional RC, the ORC extracts and generates electrical energy out of low-grade heat.

1.4.5 APPLICATIONS OF ORCS

The ORC has the ability to generate mechanical as well as electrical power in the following ways:

1.5.1 WASTE HEAT RECOVERY

This is a procedure of extracting power as of waste heat generated by variety of industrialized processes. Regeneration is utilized to recover waste heat in certain applications. Economically it's not viable to recover waste heat when HST is very low. ORC cycle makes it simple to produce electrical power from low grade heat resources. The ORC cycle is depicted in Figure 1.6.

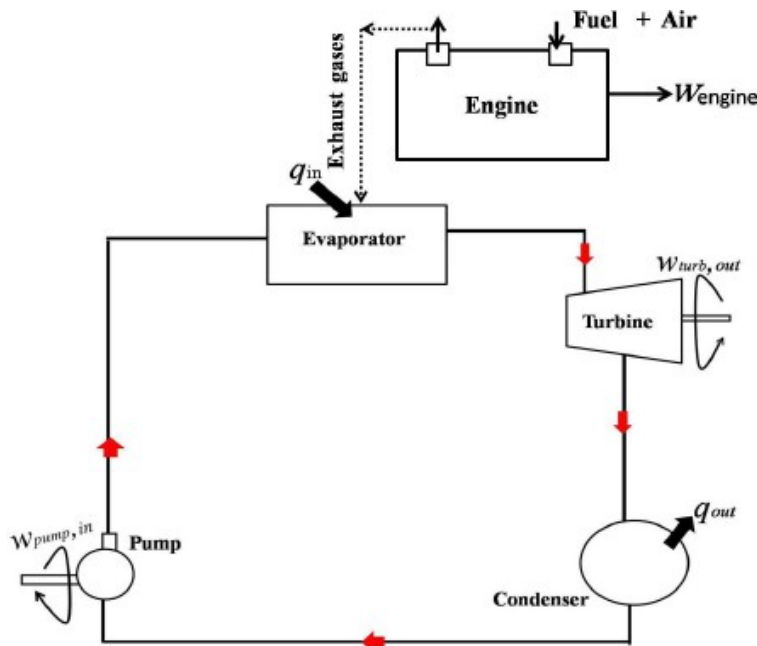


Figure 1.6 Representation of ORC

1.5.2 IN SOLAR THERMAL SYSTEM

Energy generation from Sun's energy is a technique practiced from ages. Parabolic dish, parabolic trough, as well as solar tower, can also be used to extract solar thermal energy. The parabolic dish's working temperature is between 300 and 400 degrees Celsius. This technology was coupled to the production of electric energy from steam a few years ago. The typical Rankine cycle, on the other hand, needs a source having large temperature as well as large

installation power capacity to be economically viable. The ORC operates at substantially lower temperatures and requires less cash. In comparison to the traditional Rankine cycle, the ORC demands and allows smaller component sizes. The prototype of solar thermal power plant is shown in Figure 1.7.

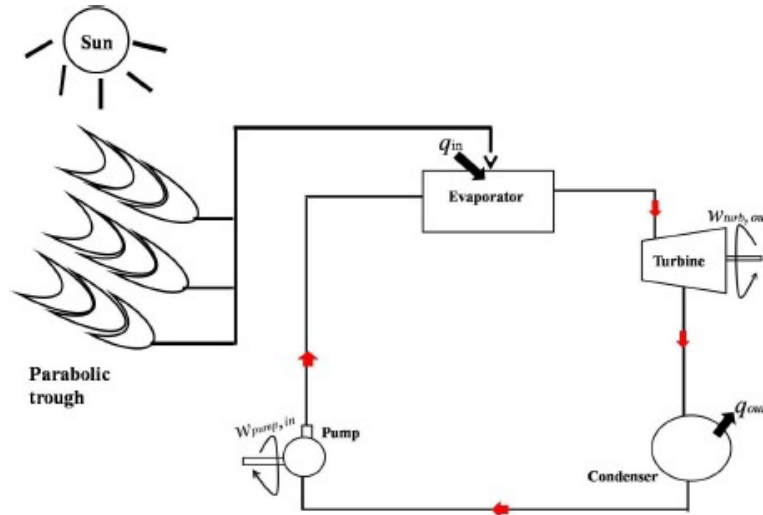


Figure 1.7 solar thermal power plants

1.5.3 BIOMASS POWER PLANT

Cost and usage of traditional fossil fuels are steadily rising. Fossil fuel consumption has a significant impact on the environment, creating climate change and pollution. Biomass energy sources are currently witnessing increased market expansion due to the fact that they are less expensive and more environmentally friendly than fossil fuels. Biomass fuels come in a variety of forms, including biogas from wood waste as well as combustible agriculture wastes. When it comes to fuel pricing and global warming potential, utilizing biomass fuels has a lot of advantages. Figure 1.8 depicts the ORC in action using biomass.

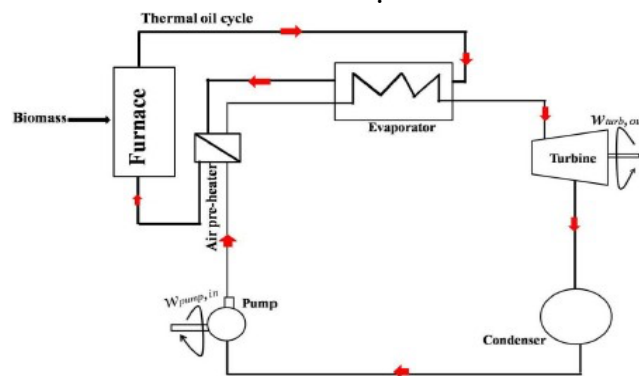


Figure 1.8 The ORC in action using biomass.

1.5.4 GEOTHERMAL POWER PLANTS

Geothermal energy provided 1% of the world's electrical power in 2008 [7]. The energy source for geothermal power plants is both renewable and clean. Flash steam, binary cycle, and dry steam power plant are three different methods that can be rummage-sale to produce electricity under this category. The geothermal power production for the dry and flash steam systems is depicted in Figure 1.9

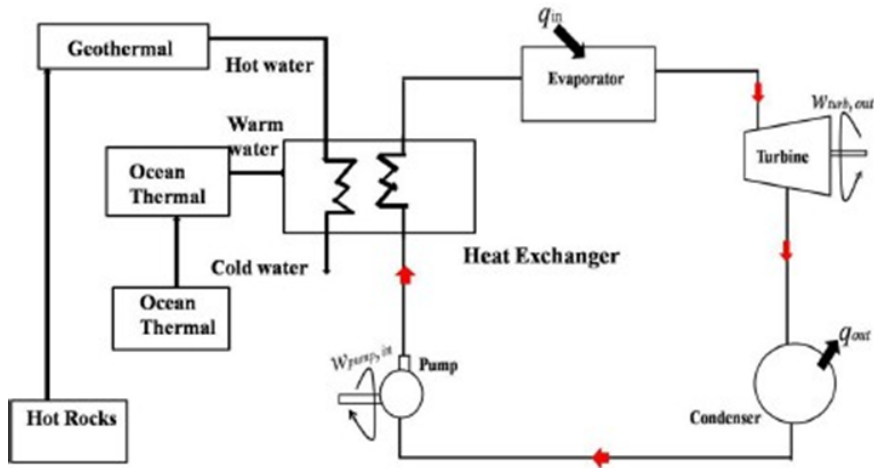


Figure 1.9 Representation of GEES

1.6 MARKET SHARE FOR DIFFERENT HEAT SOURCES

Geothermal and Biomass energy sources are the leading segments for integration. Unused heat recovery, that is now ranked IIIrd, controls 20% of ORC arcade and can be used in a variety of industrial processes. Due to a lack of knowledge, solar ORC is currently ranked fourth, through only 1% of ORC marketplace, and has a significant prospective for growth. Market share for various heat sources is depicted in Figure 2.10. Since it is the only established machinery can produce equal to 1MWel for distributed systems as of solid fuels alike biomass, biomass-based ORC has the largest application. Almost 200 plants with power production capacity of around 2000 MW are working since ORC became available commercially in the 1980s [7]. This is one of the primary reasons behind ORC's growing popularity in current years.

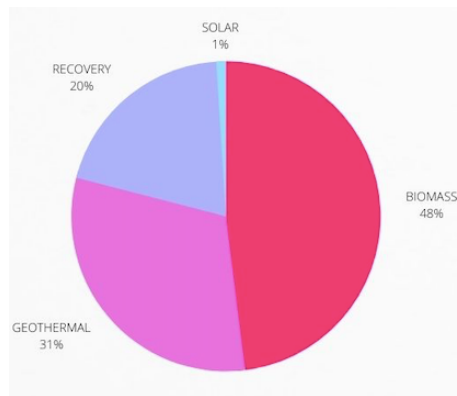


Figure 1.10 ORC market share

1.7 THE ORC AND THE CONVENTIONAL CYCLE

Factors' creating distinctions betwixt Organic Rankine Cycle and the conventional one has been discussed below.

1.7.1 OPERATIONAL FLUIDS

Basic difference among ORC and traditional steam Rankine cycle, aside from operating factors like temperature and pressure, are working substance secondhand in every cycle. Water being still the WF which can be rummage-sale in a traditional RC, but an ORC can employ over a hundred other working fluids. The search for new suitable fluids for the ORC system is never-ending. Thermodynamic property of the working fluid determines the component sizes of an ORC system. Each working fluid has different thermodynamic, environmental, and safety qualities. Most working fluids do not have publicly available safety and environmental data.

Environmental and Safety Properties

Water is an environmentally friendly working fluid since various organic fluids are unfriendly to the environment because they have the ability to deplete ozone and induce the greenhouse effect, which is hazardous to the ecosystem. High toxicity and flammability are characteristics of certain organic working fluids.

1.7.2 NORMAL BOILING POINT (NBP)

Most of the Organic Rankine Cycle WFs have lower NBP than Water. Organic WFs have three various saturated vapor line slopes, that are positive, negative and infinite slopes. For positive slope the WFs exist the expander as superheated vapor thus reducing danger of erosion. On a T-s diagram, water has a negative saturation vapor line slope, but organic working fluid has three various saturation vapor line slopes: infinite, positive, and negative. This brings down the cost

of ORC as there is no need to superheat the WF before expansion which allow us to use smaller and less expensive ORC components [8].

1.7.3 CONDENSER PRESSURE

Most ORCs have higher condensing pressures than the atmospheric pressure, (P_{atm}). This reduces the chances of infiltration at the condenser and thus increases the cycle's performance and efficiency. Organic WFs like R11, Isobutene, and R236fa, have condensing pressures of 105.49, 349.14, and 271.04kPa at a temperature of 298 K, respectively, while water has a condensing pressure of 3.15kPa [8].

1.7.4 WORKING OF SELECTED FLUID

Heat source and heat sink temperature plays a crucial role in WFs selection. For various operating conditions, in present many organic fluids that have a suitable connection b/w both heat source as well as heat sink temperature. The working fluid's thermodynamic, safety, and environmental qualities all play a role in the fluid selection process. Hence, It is not an easy task to select right fluid for an ORC. When choosing a good working fluid for ORCs, there are a few things to consider.

1.8 THERMODYNAMICE PROPERTIES

In the ORC design process, thermodynamic properties are crucial. Some of the aspects that influence ORC design are listed below.

- The heat transmission b/w organic working fluids, the heat sources, and the heat sinks temperature should be increased.
- The ambient pressure should be lower in comparison to the condensing pressure to avoid leakage difficulties, and network out in expander should be high when there is a considerable variation in enthalpy.
- Isentropic, wet, as well as dry are three organic WFs utilized in ORCs in terms of saturation vapour line slope. Wet fluids in ORCs have a -ve saturation vapour line slope, affecting liquid droplet to develop, those can impairment the turbine blades or lower their performance. Dry and isentropic working fluids do not form liquid droplets when utilized in ORCs with positive or infinite saturation vapour line slopes, because they exit the evaporator as superheated vapour. T-s diagrams significant to isentropic, moist, and dry WFs are shown in Figures 3.2 - 3.4 [9].

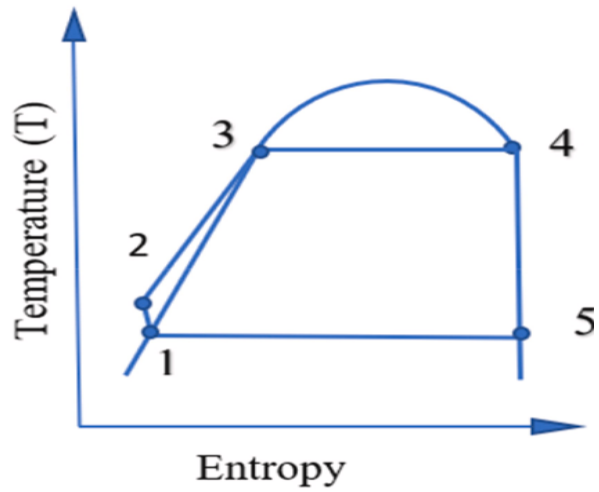


Figure 1.11 Representation of T-S diagram (isentropic working fluid)

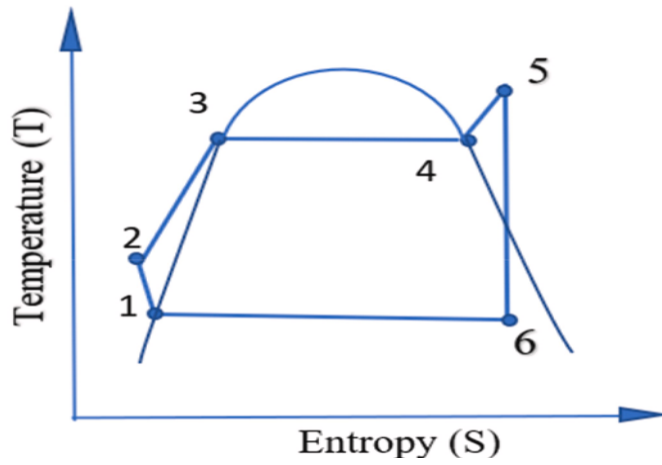


Figure 1.12 Representation of T-S diagram (Wet working fluid)

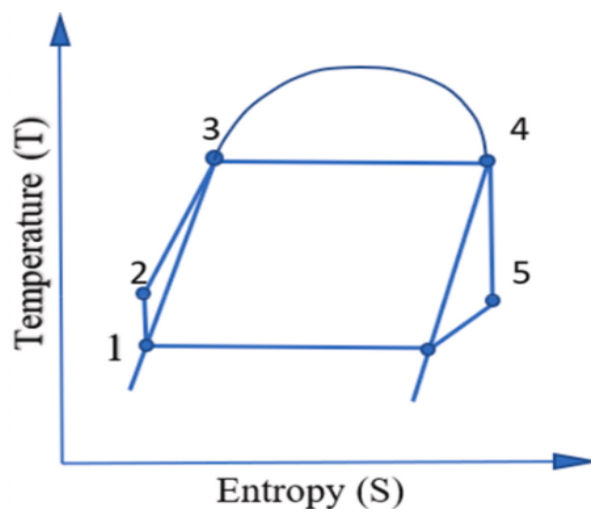


Figure 1.13 Representation of T-S diagram (dry working fluid)

1.9 CRITERIA FOR SAFETY AND THE ENVIRONMENT

Whenever choosing a working fluid, keep in mind that safety and environmental effect are important factors to consider. Many WFs have been phased out in recent years resulting in negative environmental effects, and many additional WFs has been opted out as well. The majority of WFs are being phased out because of their high GWP as well as ODP. This is crucial to remember that though certain working solutions have excellent thermal properties, they cannot be appropriate when safeties as well as atmospheric concerns are taken interested in account. Some CFCs and HCFs are example of working fluids that have been discontinued out. Certain working fluids were prohibited primarily because they cause global warming and/or ozone depletion. The following are some of the safety and environmental elements to consider while choosing a suitable working fluid: This study's safety and environmental data comes from James M. Calm's physical, safety, and environmental data [8].

Global Warming Potential (GWP)

GWP value represents global warming induced via specific working fluids in comparison to CO₂ during a 100-years period. CO₂ has a GWP of 1 while water has none. CO₂ has a significant clear effect on global warming, which is why it is utilized by way of baseline.

Ozone Depletion Potential (ODP)

In comparison to tri-chlorofluoro-methane, ODP refers to ability of an operational fluid to abolish ozone layer above the earth's surface. CFC-11 has an ODP of one, where the ozone depletion potential of other CFCs and HCFCs ranges from 0.01 to 1.0. Halons (synthetic chemical compounds comprising 1 or 2 carbon atoms and bromine) have a more ozone depletion potential, up to 10. The ODP is a very significant component to consider while choosing a working fluid. Because of their high ODP, the Montreal Protocol has phased out many working fluids. As a result, any WF chosen should have a very low ODP.

2.1 INTRODUCTION

Because of increase in greenhouse gas emissions, energy efficiency as well as conservation is gathering steam. Increasing energy consumption forces researchers to create technologies that are both energy efficient and environmentally benign, as well as commercially viable. Thermal system integration (hybrid systems) enhances energy efficiency, fuel utilization factor, and carbon emissions. Decentralized applications benefit from the integration of renewable energy sources. However, the hybrid systems' practical constraints include their initial capital cost and complexity. It is important to screen numerous alternatives prior to the detailed design of hybrid system. Therefore, the comprehensive literature review has been done to understand the level of activity like, design, modeling, and optimization of the hybridsystems with main attention on replacing conventional cooling system.

2.2 ORGANIC RANKINE CYCLE BASED HYBRID SYSTEMS

Growing interest in low-grade heat recovery for power generation or cogeneration has given more attention to ORC due to its lower evaporation temperature and simplicity (Lee et al., 2014; Yu et al., 2016) [9]. An ORC outperforms steam turbine in the range of 150-200°C HST. The combined generation of heat and power using an ORC enhances the utilization of energy and reduces the carbon emission. Organic Rankine cycle, which uses organic working fluid instead of water in the conventional Rankine cycle, efficiently utilizes low-medium temperature energy sources, like waste heat, solar thermal (Desai and Bandyopadhyay, 2016) [10], geothermal, biomass combustion, ocean thermal energy [11], etc. For <1 MWe scale low-temperature operations ORC is a promising option compared to steam Rankine cycle (Desai and Bandyopadhyay, 2016) [12].

Commercial manufacturers of ORC power block have installed significant number of plants with waste heat, biomass, or geothermal as an energy source (Quoilin et al., 2013) [13]. Many academics have looked on ORC-based cogeneration systems that use various energy sources.

Integration of an ORC in small-scale hybrid system (electric output 1–200 kWe) is a promising option due to superior thermodynamic and economic performance (Maraver et al., 2013a) [14]. Extensive investigations on organic Rankine cycle based hybrid systems powered by waste heat (Wang et al., 2011) [15], solar thermal energy using parabolic trough collector (PTC) (Al-

Sulaiman et al., 2011) [16] and flat plate collector (Wang et al., 2012) [17], solid oxide fuel cell (SOFC) (AlSulaiman et al., 2011) [18], biomass (Al-Sulaiman et al., 2012) [19], gas turbine exhaust (Ahmadi et al., 2012) [20], combined biomass and solar thermal energy (Karellas and Braimakis, 2016) [21], combined geothermal and solar thermal energy (Buonomano et al., 2015) [22] have been reported in literature. Many researchers have analyzed ORC based hybrid system using VARS, VCRS and other cooling system, like, liquid desiccant cooling system and ejector cooling system (Wang et al., 2012), as cooling unit [23].

2.3 ORC BASED HYBRID SYSTEMS RUNNING ON WASTE HEAT/THERMAL ENERGY

Energy sectors waste a lot of energy by using traditional fuels. In this regard, researchers have been trying to use waste heat as alternative energy source to produce useful commodities (Javan et al., 2016) [24]. Hybrid systems allow waste heat to be recovered in thermal systems, improving efficiency and making systems more cost effective. Many researchers have investigated ORC interconnected VARS based hybrids using waste heat as an energy source. Ahmadi et al. (2012) used waste heat energy of gas turbine to run the ORC integrated VARS and reported 89% and 55% energy and exergy efficiency, respectively [25]. Chaiyat and Kiatsiriroat (2015) focused on feasibilities of energy, economic and environment aspects of diesel burner-based waste heat powered ORC with absorption cooling system and reported 10 years of payback period [26]. Fang et al. (2012) recovered waste heat-based combine ORC, VARS, and coil-based heating system for dynamically adjustable electricity to thermal energy ratio [27]. VCRS has also been used to investigate waste heat ORC systems. Wang et al. (2011a) integrated micro scale ORC with VCRS and reported overall COP about 0.48 [28]. Wang et al. (2011) analyzed hybrid ORC-VCRS with sub cooling as well as with sub cooling and recuperation [29]. The reported overall COP is 0.54 with basic VCRS, 0.63 with sub cooling, and 0.66 with sub cooling and recuperation. Moles et al. (2015) analyzed low temperature ORC powered VCRS based hybrid system for different low GWP working fluids and reported payback period of 3.3 years [30]. Dai et al. (2009) analyzed waste heat (composed of 96.16% N₂, 3.59% O₂, 0.23% H₂O, and 0.02% NO+NO₂ by volume) energy powered ORC integrated ejector refrigeration cycle and reported thermal and exergy efficiency about 13% and 22%, respectively [31]. Javan et al. (2016) utilized waste heat of diesel engine to run the ORC based ejector refrigeration cycle and carried out fluid selection optimization for residential applications [32]. Yang et al. (2016) analyzed ORC integrated ejector cycle using zeotropic mixture isobutane/pentane with 0.4%, 0.7% and 0.8% mass fraction [34].

2.4 ORC BASED HYBRID SYSTEMS POWERED BY SOLAR-THERMAL ENERGY

Researchers have been working on refining solar energy thermodynamic cycles and developing new ones to address environmental issues in recent years. In different thermodynamic cycles, various solar technologies such employed. Because the ORC has a lower evaporation temperature, a lot of researchers have combined low temperature solar technology with it. Various cooling methods, such as VCRS, VARS, and ejector cooling systems, are used in solar-ORC hybrid systems. For example, Al- Sulaiman et al. (2011a) integrated PTC, ORC and VARS to generate combine cooling, heating and power [35]. Al-Sulaiman et al. (2011) reported overall efficiency for organic Rankine cycle-based hybrid systems powered by solar thermal energy (90%), solid oxide fuel cell (76%), and biomass (90%) [36]. Suleman et al. (2014) analyzed integrated solar geothermal cycle where solar powered ORC integrated with VARS for cooling along with the drying process and geothermal powered ORC for power generation. The system/cycle has total energetic and exergetic efficiencies of 54.7 percent and 76.4 percent, respectively [37]. Buonomano et al. (2015) performed thermodynamic and economic analysis of micro scale ORC powered VARS using combine source of solar-thermal and geothermal [38]. Karellas and Braimakis (2016) analyzed solar (using PTC)-biomass energy powered ORC integrated VCRS system with R134a, R152a, R245fa working fluids in the system [39]. Chang et al. (2017) analyzed hybrid proton exchange membrane fuel cells (PEMFC) energy power ORC with compression system [40]. The performance evaluation and fluid selection of an ORC integrated vapour compression chiller for ice production was done by Bu et al. (2013) [41]. Among the R123, R245fa, R600a, & R600 working fluids tested, R123 proved to be the best suited for the ORC-VCC pair [42]. Wang et al. (2012) analyzed flat-plate collector powered ORC integrated ejector refrigeration cycle for different modes, like combine power and cooling, combine power and heating and power mode [43]. Boyaghchi and Heidarnejad (2015) analyzed solar evacuated tube collector-based ORC integrated ejector cooling unit and reported 23.7% energy efficiency and 9.5% exergy efficiency during summer mode [44]. Rostamzadeh et al. (2017) investigated performance of solar energy powered ORC integrated ejector refrigeration cycle and reported R123/isobutene as most appropriated fluid pair among R123, R245fa, and isobutane ORC working fluids [45].

2.5 ORC BASED HYBRID SYSTEMS RUNNING ON BIOMASS ENERGY

Biomass-backed renewable energy has the potential to decrease the use of fossil fuel or their harmful effects on the environment. Energy can be extracted from waste biomass using a variety of processes and technologies. In comparison to typical fossil fuel-based systems, biomass energy-based hybrid systems have a lower carbon footprint and lower energy costs. Because biomass-fueled power systems are inefficient, they are frequently combined with heating or cooling systems for improving overall efficiency. Many studies have combined biomass-powered organic Rankine power cycles with various cooling cycles, such as VCRS, VARS, ejector systems, and desiccant units.

Al-Sulaiman et al. (2012) analyzed 500 kW ORC integrated absorption unit for combined cooling, heating and power applications and reported 89% energy efficiency and 28% exergy efficiency [46]. Huang et al. (2013) carried out techno-economic analysis of a small-scale biomass-driven ORC integrated absorption cooling system. The variation in efficiency is within the range of 1% for power mode, 5% for combined heat and power mode, and 4% for trigeneration mode. Maraver et al. (2013) investigated various organic WFs for biomass supported hybrid systems on a small and large scale. R245fa, R134a, and R152a are ideal for condensing temperatures of 20 to 35°C and relevant elements; n-pentane, toluene, and slogans, on the other hand, are best for condensing temperatures of 60 to 80°C and large-scale applications [47]. Amirante et al. (2016) performed energetic and economic analysis of biomass based hybrid system which comprises commercially available 280 kW organic Rankine cycle unit and absorption chiller for air conditioning of airport building [48].

Karellas and Braimakis (2016) used combine biomass-solar energy source for ORC integrated compression unit for micro scale applications. The system was tested with R134a, R152a, and R245fa WFs, and a 7-year payback period was observed [49]. Jradi and Riffat (2014) experimentally investigated micro-scale biomass-based hybrid system using liquid desiccant cooling system and reported overall efficiency of 83% for combined heat and power mode and 85% for regenerations [50].

2.6 ORC BASED HYBRID SYSTEMS RUNNING ON GEOTHERMAL ENERGY

Geothermal energy can provide power, heat, and cool depending on the source temperature and can be used in a variety of applications such as industrial drying, distillation, as well as desalination. The combination of a low-temperature geothermal source and an ORC provides enormous power generation potential. Only limited investigators have combined geothermal ORC using other cooling systems.

Suleman et al. (2014) developed hybrid cycle based on two ORC units powered by solar energy (for power generation, drying process and VARS based cooling) and another ORC runs on geothermal energy for power generation [51]. Zare (2016) performed thermodynamic optimization of ORC integrated absorption cycle for regenerations application and reported isobutene as a promising working fluid compared to n-pentane, R245fa, and R152a [52]. Akramiet al. (2017) carried out energetic and Exergo-economic assessment of geothermal ORC integrated absorption cycle and reported 35% energy efficiency and 49% exergy efficiency [53].

2.7 ORGANIC RANKINE CYCLE ON A MICRO SCALE

On a small and micro scale, growing interest in the organic Rankine cycle has corresponded with rising power use and carbon emissions. ORC based on renewable thermal energy is also gaining popularity as a means of generating decentralized electricity. Furthermore, ORC plants do not require an on-site operator. There are no producers of small and medium ORC units in India. As a result, ORC systems have not penetrated the Indian market. The implementation of indigenous ORC would be a cost-effective solution because it lowers both the leveled and specific investment costs of energy.

The claimed expander isentropic efficiency range is around 40-80 percent, resulting in a thermal efficiency of 3-14 percent for the cycle. Wide variances in cost data are commonly reported in theoretical analyses for various capacities of ORC systems. The cost of the micro scale ORC power block is estimated to be between 2264 and 4516 USD/kWe as well as 1080-6360 USD/kWe (Quoilin et al., 2011) [54].

2.8 PRESENT WORK

The performance of ORC is studied utilizing four different WFs (R32, R600a, R134a, and RC318) while considering steady outer constraints. The first and second law efficiencies, TSF and Net-work output have been parametrically compared with varying TIT, heat source temperature, turbine efficiency, temperature differential between the pinch points.

2.9 OBJECTIVES OF STUDY

The objective of this paper is to analyze the effect of heat source temperature, TIT, PPTD and turbine efficiency on Thermal efficiencies, TSF and Net Work Output while using four WFs of which two (RC318, R600a) belong to dry fluids category and other two (R134a, R32) belong two wet fluids category. The simulation program is being developed on EES to analyze the performance parameters.

3.1 SYSTEM MODELING

It is required to implement Physical model in a mathematical model to aid in the analysis of engineering problems. To achieve the objective state point equations for thermodynamic characteristics is developed and after that, using software or directly from the reference, polynomial for thermodynamic properties is developed.

As a result, physical equations, mass, and energy balance, expectation as well as state point equation, and thermal properties are all covered in this chapter.

3.2 SYSTEM DESCRIPTION

3.2.1 WORKING PRINCIPLE AND MATHEMATICAL MODEL OF ORC

Figure 3.1 depicts the ORC analyzed in this work. Procedure 1 to 2 (Pressure increase in pump), procedure 2 to 3 (heat addition in evaporator), procedure 3 to 4 (Expansion of gas in turbine), and procedure 4 to 1 are the four processes (heat rejected in condenser).

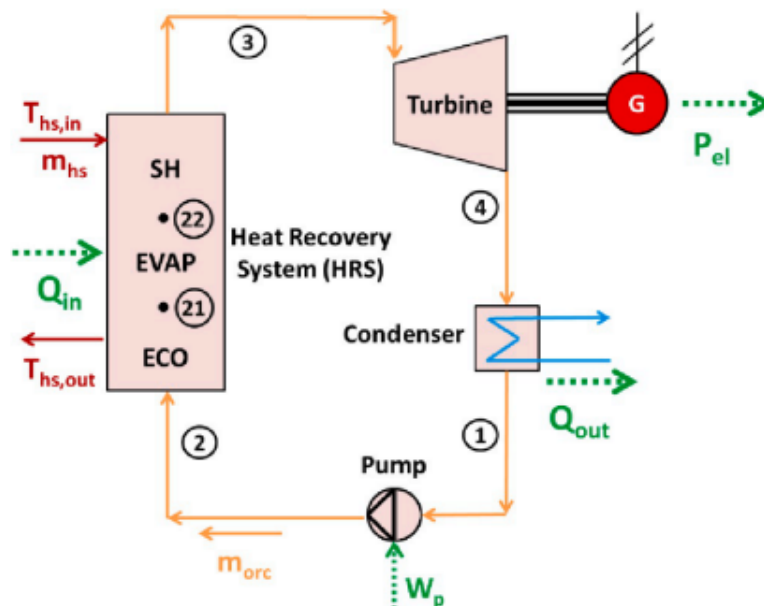


Figure 3.1 Schematic representation of ORC

The assumptions considered for this study are,

- (1) steady state operating conditions are considered.
- (2) pressure drop and heat losses are neglected.
- (3) Kinetic energy and potential energy changes are neglected.
- (4) WFs come out as saturated fluids from evaporator and condenser

3.4 MATHEMATICAL MODELLING

Engineering Equation Solver is used to design and implement modelling equations. Following general assumptions underpin the computer modelling. In heat exchanger as well as tube, pressure drops is minimal. Working fluids in VCC is saturated vapor when it goes into compressor or saturated liquid when leaving condenser. VCC's expansion is an adiabatic process. The ORC subsystem has no effect on the AC subsystem's specified condensation temperature. The ORC's working fluid exit at condenser as a saturated fluid or enters in to turbine as a saturated vapor.

Mass balance

$$\sum_{in} \dot{m} = \sum_{out} \dot{m} \quad (1)$$

Energy balance:

$$Q - W = \sum_{out} \dot{m} h - \sum_{in} \dot{m} h \quad (2)$$

Net power output of ORC system (W_{net}) is evaluated using Eq.

$$W_{net} = W_{turbine} - W_{pump} \quad (3)$$

$$W_{pump} = \frac{\dot{m}(h_4s - h_3)}{\eta_{pump}} \quad (4)$$

$$W_{turbine} = (h_1 - h_{2s})\dot{m} \times \eta_{Turbine} \quad (5)$$

The first and second law efficiencies of ORC (η_I , η_{II}) were calculated using Eq.

$$\eta_I = \frac{W_{net}}{Q_{in}} \quad (6)$$

$$\eta_{II} = \frac{W_{net}}{\left[\frac{Q_{in}(1-T_o)}{T_m} \right]} \quad (7)$$

TSF also directly proportional to turbine size was determined using Eq.

$$TSF = \frac{\sqrt{V_2}}{\Delta H_{is}^{\frac{1}{4}}} \quad (8)$$

In this research, a thermodynamic model was created using Engineering Equation Solver software, and the findings of the research are presented in the sections below.

The input conditions that were used in the study are listed below.

Input Parameters	Value
Condenser temperature ($T_{condensor}$)	28°C
Evaporator temperature ($T_{evaporator}$)	120°C
Turbine and evaporator isentropic efficiency	0.9
Mass flow rate of heat source fluid	1.2kg/s

4.1 EFFECTS OF HEAT SOURCE TEMPERATURE

The Ist law and IInd law efficiency as well as TSF of ORC has been analyzed employing R32, R600a, R134a, and RC318 such as working fluid using parametric analysis. To predict thermodynamic performance of ORC with varied heat source temperature, a computer model in Engineering Equation Solver (EES) was built.

Figures 4.1-4.3 depict First Law efficiency as function of source temperature.

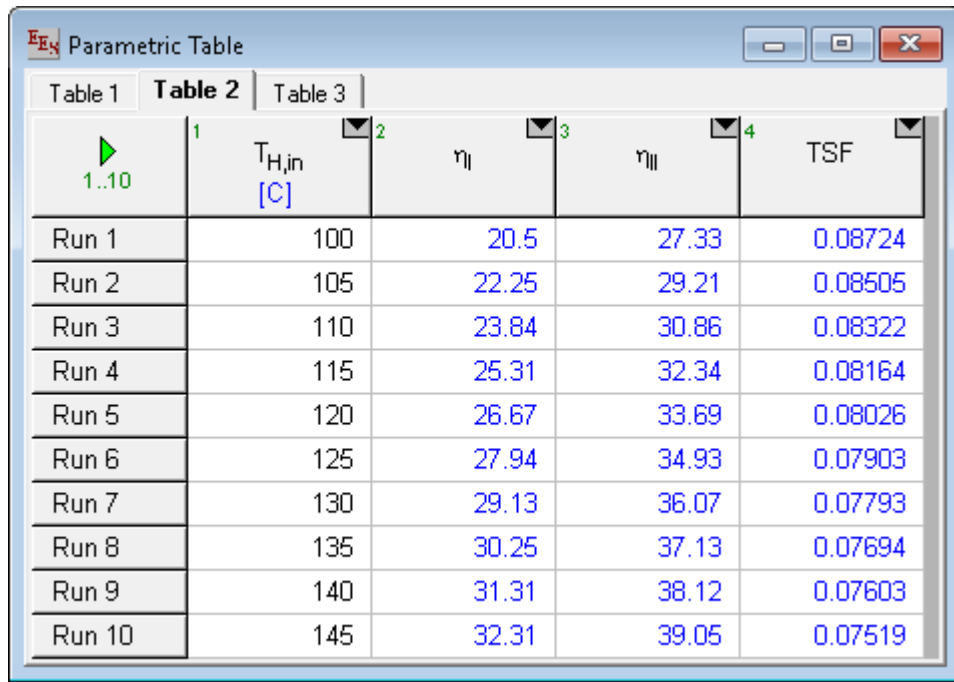
Table 4.1: Simulations results using R32

	1	2	3	4	
▶ 1..10	$T_{H,in}$ [C]	η_I	η_{II}		TSF
Run 1	100	22.29	29.72		0.05447
Run 2	105	23.45	30.78		0.0537
Run 3	110	24.55	31.77		0.05302
Run 4	115	25.6	32.72		0.05239
Run 5	120	26.61	33.61		0.05183
Run 6	125	27.57	34.47		0.05131
Run 7	130	28.5	35.28		0.05083
Run 8	135	29.38	36.06		0.05038
Run 9	140	30.24	36.81		0.04997
Run 10	145	31.06	37.53		0.04959

Table 4.2: Simulations results using R600

	1	2	3	4	
▶ 1..10	$T_{H,in}$ [C]	η_I	η_{II}		TSF
Run 1	100	15.34	20.45		0.1257
Run 2	105	16.91	22.19		0.1223
Run 3	110	18.37	23.77		0.1194
Run 4	115	19.75	25.23		0.117
Run 5	120	21.04	26.58		0.1148
Run 6	125	22.27	27.84		0.1129
Run 7	130	23.44	29.02		0.1112
Run 8	135	24.55	30.13		0.1097
Run 9	140	25.61	31.18		0.1083
Run 10	145	26.62	32.17		0.107

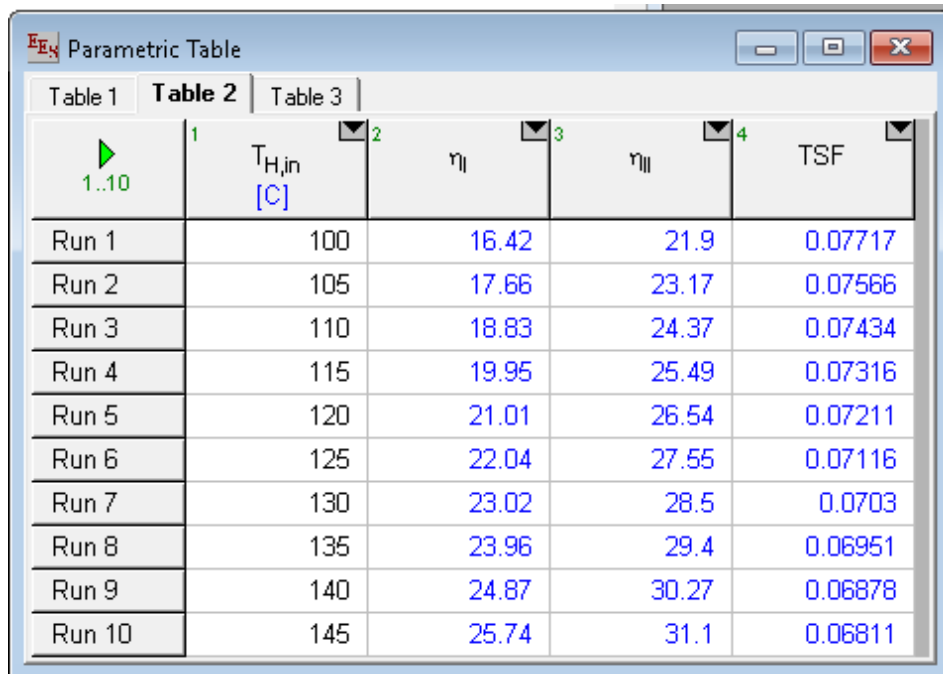
Table 4.3: Simulations results using R134a



The screenshot shows the EES Parametric Table window for R134a. The window title is "EES Parametric Table". It has three tabs: "Table 1", "Table 2", and "Table 3". "Table 2" is selected. The table has five columns: a play button with "1..10", $T_{H,in}$ [C], η_I , η_{II} , and TSF. The rows are labeled "Run 1" through "Run 10".

	1	2	3	4	
	$T_{H,in}$ [C]	η_I	η_{II}	TSF	
Run 1	100	20.5	27.33	0.08724	
Run 2	105	22.25	29.21	0.08505	
Run 3	110	23.84	30.86	0.08322	
Run 4	115	25.31	32.34	0.08164	
Run 5	120	26.67	33.69	0.08026	
Run 6	125	27.94	34.93	0.07903	
Run 7	130	29.13	36.07	0.07793	
Run 8	135	30.25	37.13	0.07694	
Run 9	140	31.31	38.12	0.07603	
Run 10	145	32.31	39.05	0.07519	

Table 4.4: Simulations results using RC318



The screenshot shows the EES Parametric Table window for RC318. The window title is "EES Parametric Table". It has three tabs: "Table 1", "Table 2", and "Table 3". "Table 2" is selected. The table has five columns: a play button with "1..10", $T_{H,in}$ [C], η_I , η_{II} , and TSF. The rows are labeled "Run 1" through "Run 10".

	1	2	3	4	
	$T_{H,in}$ [C]	η_I	η_{II}	TSF	
Run 1	100	16.42	21.9	0.07717	
Run 2	105	17.66	23.17	0.07566	
Run 3	110	18.83	24.37	0.07434	
Run 4	115	19.95	25.49	0.07316	
Run 5	120	21.01	26.54	0.07211	
Run 6	125	22.04	27.55	0.07116	
Run 7	130	23.02	28.5	0.0703	
Run 8	135	23.96	29.4	0.06951	
Run 9	140	24.87	30.27	0.06878	
Run 10	145	25.74	31.1	0.06811	

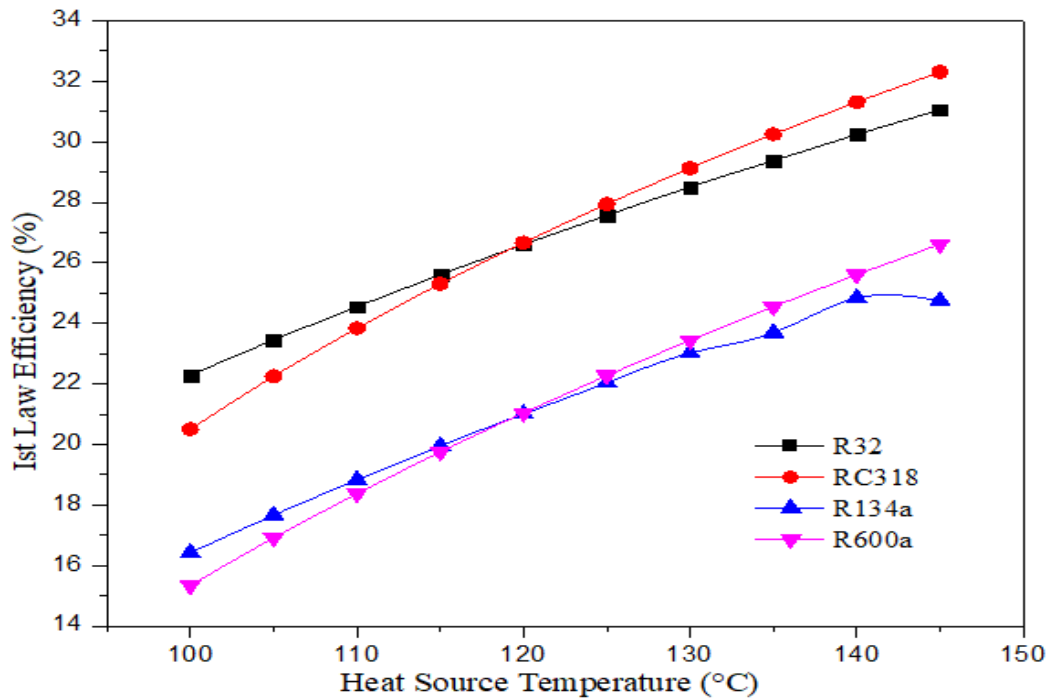


Figure 4.1 First law Efficiency vs HST

Influence of heat sources temperature in ORC's 1st law effectiveness is shown in Fig. 4.1(b). Similar trend is found in variation of 1st law efficiency for all the four WFs. It demonstrates a monotonic increase of First law efficiency with rising heat source temperature. 1st law efficiencies increased 40.12% for R32, 74.49% for R600a, 58.85% for R134a, and 59.70 % for RC318 as TIT rises from 100 to 145 °C with a step of 5°C. The best thermal efficiency is achieved by RC318; it is followed by R32, R600a, and R134a.

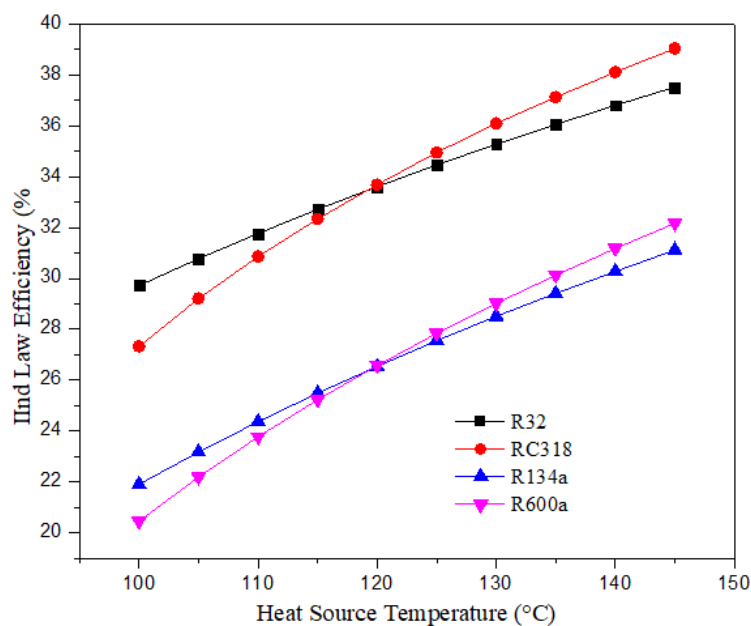


Figure 4.2 Efficiency of the second law as a function of HST

Fig. 4.2 depicts IInd law efficiency as a function of HST. It demonstrates a monotonic increase in IInd law efficiency for all the WFs in consideration with increasing heat source temperature. The IInd law efficiencies increased 40.01% for R32, 75.44 % for R600a, 58.55 % for R134a, and 59.52% for RC318 as TIT rises from 100 to 145 °C with a step of 5^o. The best thermal efficiency is achieved by RC318; it is followed by R32, R600a, and R134a.

The reason is that as the mean temperature of heat addition increases the cycle irreversability decreases which in turn increases the cycle efficiency.

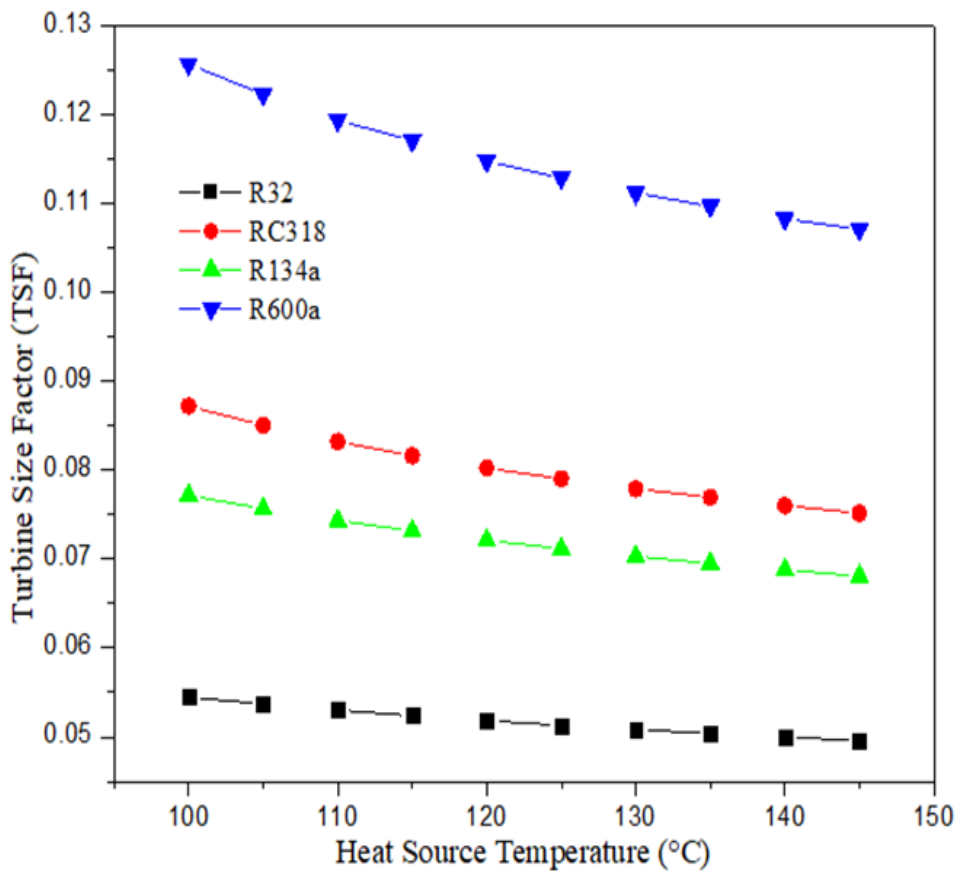


Figure 4.3 TSF vs. HST

Fig.4.3 demonstrates TSF as function of HST. With heat source getting bigger TSF gets smaller. Small size factors are achieved for R32 at maximum HSTs for the conditions under consideration. Because of low evaporation pressure, R600a needs greatest size parameter. At all of the HSTs, R32 has the smallest turbine size parameter.

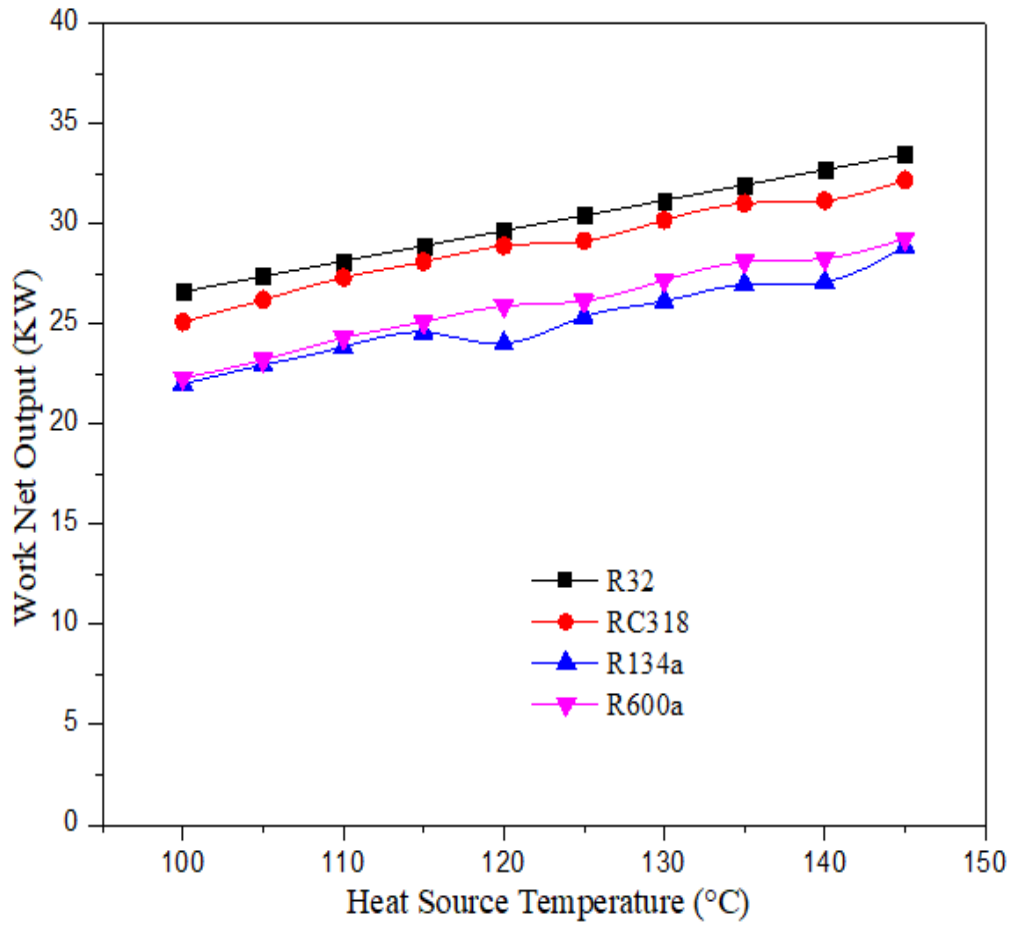


Figure 4.4: Net Work Output vs HST

Figure 4.4 depicts Net Work Output as function of HST. For the HST range of 100 to 145°C the Net Work Output increases gradually. For this case R32 has the highest Net Work output over all the temperature range of heat source followed by RC318, R600a and R134a. R134a shows the least Net Work output over all HST range. But the increase is not so significant.

This is because with increase in HST the mean temperature of heat addition increases which in turn increases the available energy and as a result Net Work Output increases.

4.2 EFFECT OF TURBINE INLET TEMPERATURE

The research is about examining Ist law, IInd law efficiency, as well as TSF of ORC employing R32, R600a, R134a, and RC318 as working fluid using parametric analysis. To predict thermodynamic analysis of using WFs at various TIT, a computer program on EES was constructed.

Table 4.5: Simulation results after variation in turbine inlet temperatures using R32

Run	T ₁ [C]	η _I	η _{II}	TSF
Run 1	100	24.55	31.01	0.05302
Run 2	130	30.24	38.19	0.04997
Run 3	160	34.74	43.88	0.048
Run 4	190	38.4	48.51	0.04661
Run 5	220	41.45	52.36	0.04557
Run 6	250	44.03	55.61	0.04477
Run 7	280	46.23	58.39	0.04413
Run 8	310	48.12	60.79	0.04361
Run 9	340	49.77	62.87	0.04319
Run 10	370	51.22	64.7	0.04283

The input parameters for the following analysis are as monitors: Mass flow rates was 1.2kg/s, heat sources temperature was 100°C; condenser temperature is 28°C; turbine or pump isentropic effectiveness were 0.90; pinch point temperature changes in evaporator and condenser were expected to be 5. In all circumstances, these input parameters remain constant. Figures 4.5-4.8 depict the results of the analysis.

Table 4.6: Simulation results after variation in turbine inlet temperatures using R600a

1..10	1 T ₁ [C]	2 η	3 η _{II}	4 TSF
Run 1	100	18.37	23.21	0.1194
Run 2	130	25.61	32.35	0.1083
Run 3	160	31.11	39.29	0.102
Run 4	190	35.5	44.84	0.09773
Run 5	220	39.11	49.4	0.09461
Run 6	250	42.13	53.21	0.09222
Run 7	280	44.68	56.44	0.09032
Run 8	310	46.87	59.2	0.08878
Run 9	340	48.75	61.58	0.08751
Run 10	370	50.38	63.64	0.08645

Table 4.7: Simulation results after variation in turbine inlet temperatures using R134a

1..10	1 T ₁ [C]	2 η	3 η _{II}	4 TSF
Run 1	100	18.83	23.78	0.07434
Run 2	130	24.87	31.41	0.06878
Run 3	160	29.67	37.48	0.06539
Run 4	190	33.63	42.49	0.06303
Run 5	220	36.97	46.7	0.06129
Run 6	250	39.82	50.3	0.05994
Run 7	280	42.28	53.41	0.05886
Run 8	310	44.43	56.13	0.05799
Run 9	340	46.32	58.52	0.05726
Run 10	370	48	60.63	0.05665

Parametric Table					
Table 1	Table 2	Table 3	Table 4		
1..10	1	2	3	4	
	T_1 [C]	η_I	η_{II}	TSF	
Run 1	100	23.84	30.12	0.08322	
Run 2	130	31.31	39.55	0.07603	
Run 3	160	36.64	46.29	0.07186	
Run 4	190	40.73	51.44	0.06903	
Run 5	220	43.97	55.54	0.06695	
Run 6	250	46.62	58.88	0.06536	
Run 7	280	48.81	61.66	0.06409	
Run 8	310	50.66	63.99	0.06306	
Run 9	340	52.24	65.99	0.06222	
Run 10	370	53.6	67.7	0.06151	

Table 4.8: Simulation results after variation in turbine inlet temperatures using RC318

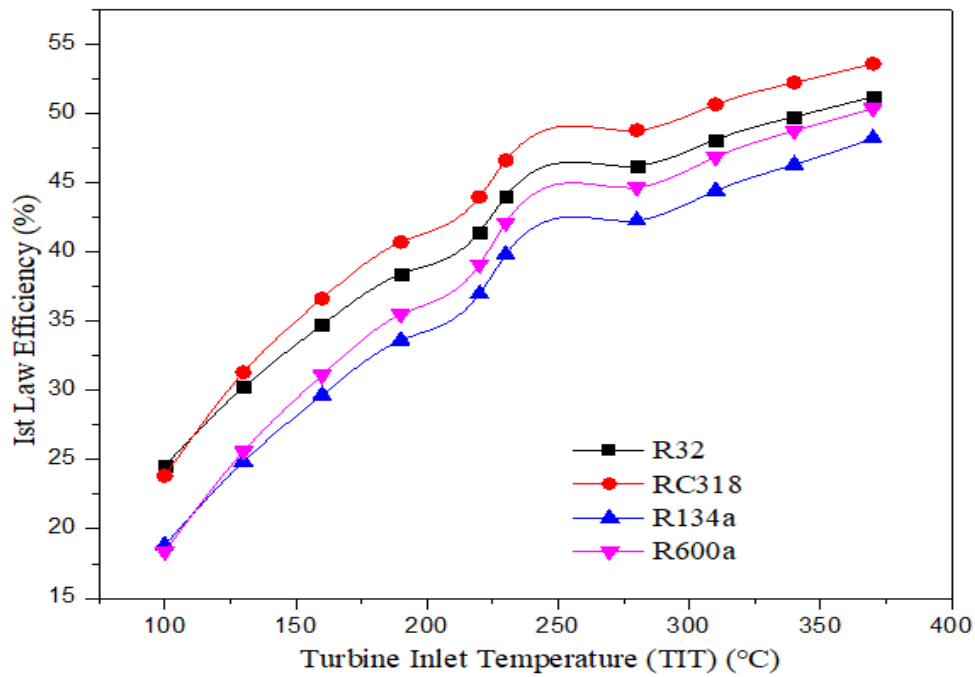


Fig. 4.5: First-law efficiency Vs TIT.

Fig. 4.5 depicts First Law Efficiency as a function of TIT. The effects of TIT on first law efficiency are found to be similar for different WFs. It depicts that when the TIT increases, the first law thermal efficiency increases in a monotonic manner. First law efficiencies for R32, R600a, R134a, and RC318 improve approximately as TIT rises from 100 to 370 °C with a step of 30°C. The best thermal efficiency is achieved by RC318; it is followed by R32, R600a, and R134a.

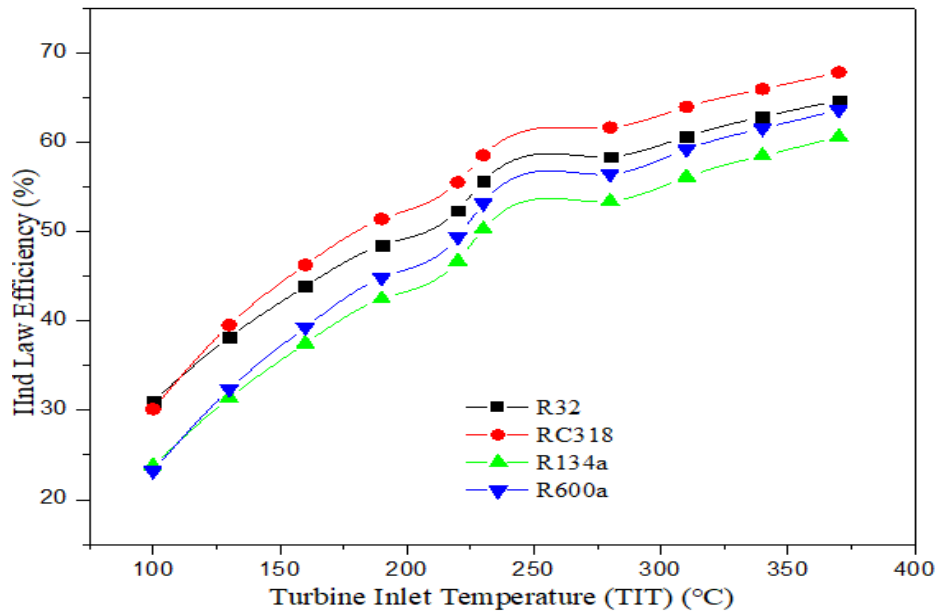


Fig. 4.6: Second Law Efficiency vs TIT

Above graph depicts IInd Law Efficiency as function of TIT. IInd law efficiency improves as TIT rises. The IInd law efficiencies for R32, R600a, R134a, and RC318 increase approximately as TIT rises from 100 to 370 °C with a step of 30°C. The best thermal efficiency is achieved by RC318; it is followed by R32, R600a, and R134a. The impacts of TIT on the ORC's turbine size factor are seen in Fig. 4.6. When the TIT is increased, turbine size factor generally drops. R32 has tiny size factors at high TITs for conditions under consideration. Because of the low evaporation pressure, R600a requires the biggest size parameter. With varying range of TITs the R134a reflects the smallest turbine size parameter.

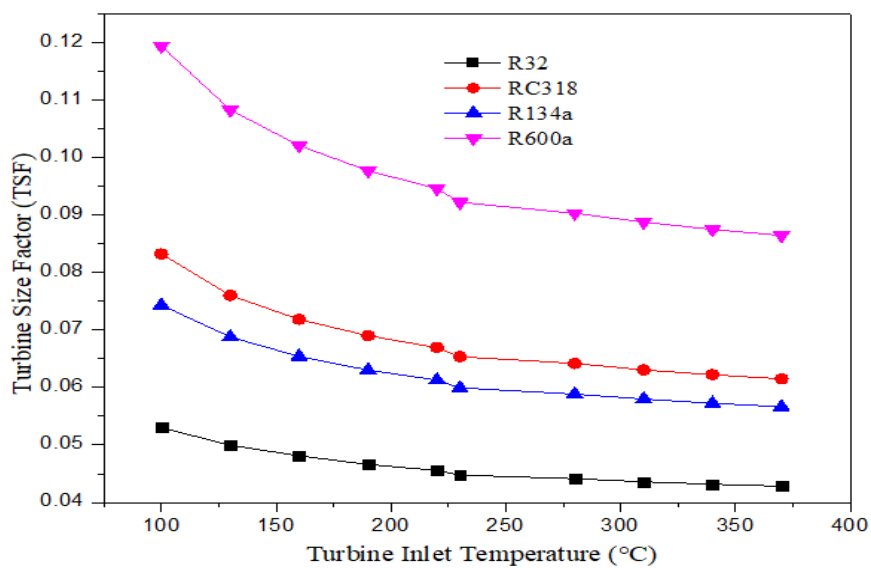


Fig. 4.7: TSF vs. TIT

The impacts of TIT on the ORC's turbine size factor are seen in Fig. 4.7. When the TIT is increased, turbine size factor generally drops. R32 has tiny size factors at high TITs for conditions under consideration. Because of the low evaporation pressure, R600a requires the biggest size parameter. With varying range of TITs the R134a reflects the smallest turbine size parameter

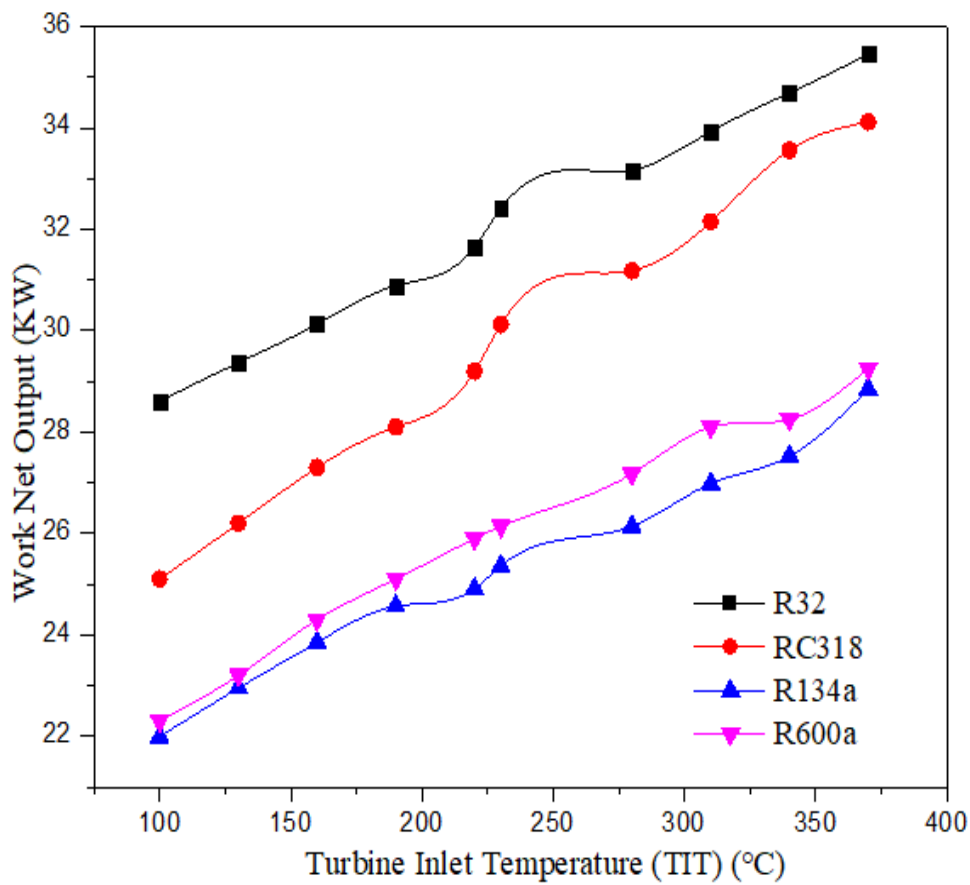


Fig.4.8: Net Work Output vs TIT

Figure.4.8 depicts Net Work Output as function of TIT. It can be inferred from the graph that for the TIT varying from 100 to 370°C with a step increase of 30°C, Net Work Output increases for all the four WFs. R32 achieves highest Net Work Output over the range of TITs while RC318, R600a, R134a trailing behind it. R134a has the minimum Net Work Output over all the range of TITs.

4.3 EFFECT OF PINCH POINT TEMPERATURE VARIANCE

Current analysis depicts the trend of Ist law efficiency, IInd law efficiency, as well as TSF of ORC employing R32, R600a, R134a, and RC318. To predict thermodynamic performance of ORC with varied pinch point temperature differences for different WFS, a computer program was built on Engineering Equation Solver (EES).

Table 4.9: Simulation results after variation in pinch point temperature difference using R32

Run	$\delta T_{ap,e}$ [C]	η_I	η_{II}	TSF
Run 1	10	26.61	33.61	0.05183
Run 2	12	26.21	33.11	0.05205
Run 3	14	25.81	32.6	0.05228
Run 4	16	25.4	32.08	0.05251
Run 5	18	24.98	31.55	0.05276
Run 6	20	24.55	31.01	0.05302
Run 7	22	24.12	30.46	0.05328
Run 8	24	23.67	29.9	0.05356
Run 9	26	23.22	29.33	0.05385
Run 10	28	22.76	28.75	0.05415

Table 4.10: Simulation results after variation in PPTD using R600a

1..10	1 $\delta T_{ap,e}$ [C]	2 η	3 η_{II}	4 TSF
Run 1	10	21.04	26.58	0.1148
Run 2	12	20.53	25.94	0.1157
Run 3	14	20.01	25.28	0.1165
Run 4	16	19.48	24.6	0.1174
Run 5	18	18.93	23.91	0.1184
Run 6	20	18.37	23.21	0.1194
Run 7	22	17.8	22.48	0.1205
Run 8	24	17.21	21.74	0.1217
Run 9	26	16.6	20.97	0.1229
Run 10	28	15.98	20.18	0.1242

Table 4.11: Simulation results after variation in PPTD using R134a

1..10	1 $\delta T_{ap,e}$ [C]	2 η	3 η_{II}	4 TSF
Run 1	10	21.01	26.54	0.07211
Run 2	12	20.59	26.01	0.07252
Run 3	14	20.16	25.47	0.07294
Run 4	16	19.73	24.92	0.07339
Run 5	18	19.28	24.35	0.07385
Run 6	20	18.83	23.78	0.07434
Run 7	22	18.37	23.2	0.07485
Run 8	24	17.89	22.6	0.07538
Run 9	26	17.41	22	0.07595
Run 10	28	16.92	21.38	0.07654

Table 4.12: Simulation results after variation in pinch point temperature difference using RC318

Parametric Table				
Table 1	Table 2	Table 3		
1..10	$\delta T_{ap,e}$ [C]	η_{II}	η_{III}	TSF
Run 1	10	26.67	33.69	0.08026
Run 2	12	26.14	33.02	0.08079
Run 3	14	25.59	32.32	0.08135
Run 4	16	25.03	31.61	0.08194
Run 5	18	24.44	30.88	0.08256
Run 6	20	23.84	30.12	0.08322
Run 7	22	23.22	29.34	0.08392
Run 8	24	22.58	28.52	0.08466
Run 9	26	21.92	27.68	0.08546
Run 10	28	21.22	26.81	0.08631

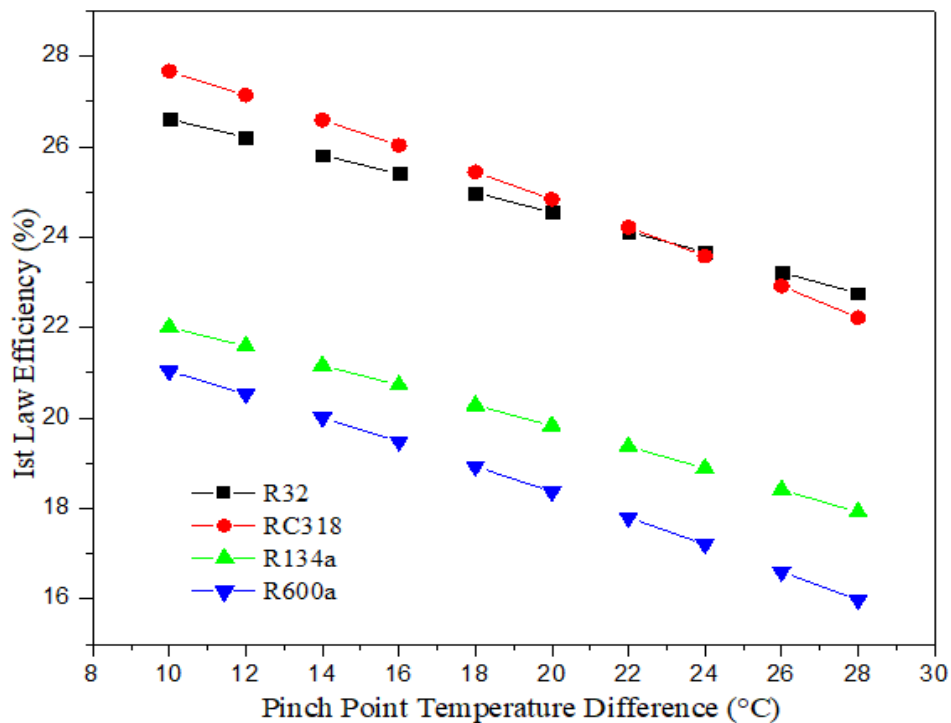


Fig. 4.9: Pinch point temperature differential vs. variation of first law efficiency

Fig.4.9 depicts Ist law efficiency as a function of Pinch point temperature difference (PPTD). The effects of varied PPTD on Ist law efficiency are shown to be same manner for different

working fluids. Ist law thermal efficiency diminishes monotonically as pinch point temperature difference increases. For PPDT in a range 10 to 28^o C the Ist law efficiency decreases for R134a, R600a, R134a, and RC 318. R32 out performs the other three WFs in terms of Ist law efficiency.

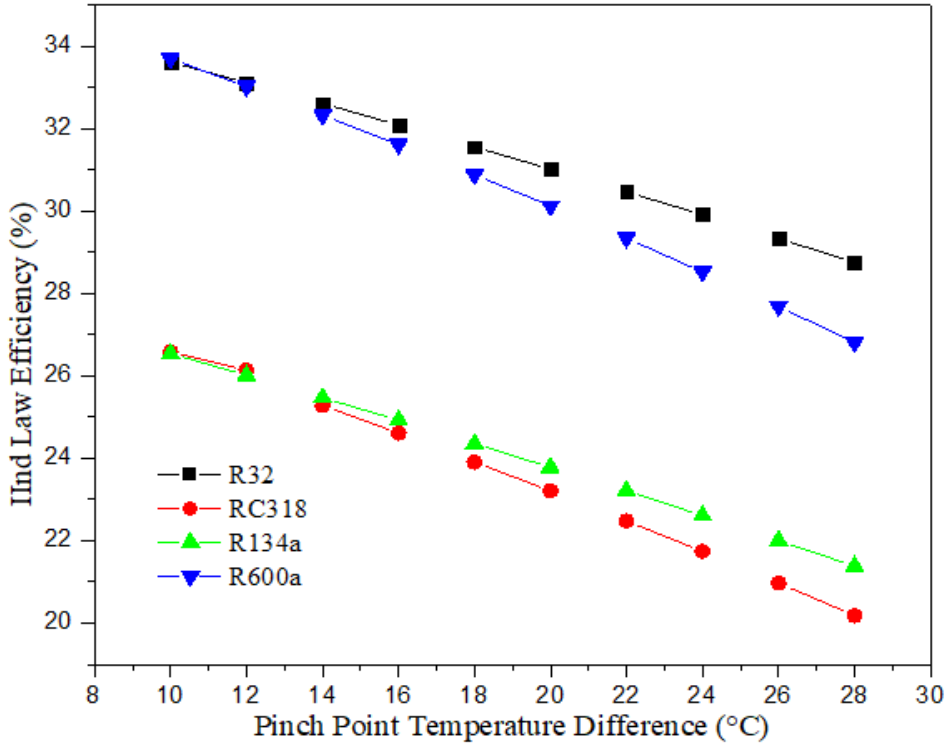


Fig. 4.10: Demonstration of pinch point temperature with respect to second efficiency

Fig. 4.10 depicts IInd Law Efficiency as a function of PPTD. The effect of varying PPTD on Ist law efficiency is shown to be same manner for different working fluids. IInd law thermal efficiency diminishes monotonically as pinch point temperature difference increases. IInd law efficiencies for R32, R600a, R134a, and RC318 decline as PPTD rises from 10 to 28°C. R32 has the maximum thermal efficiency, trailed by other three WFs.

Fig.4.12 depicts Net Work Output as function of PPTD. It can be inferred from the graph that, with increasing PPTD from 10^o to 28^o C the Net Work Output decreases. The monotonic decrease in Net Work Output can be seen for all the working fluids. R32 and RC318 shows almost the highest Net Work Output together while R134a and R600a shows the lowest Net Work Output together.

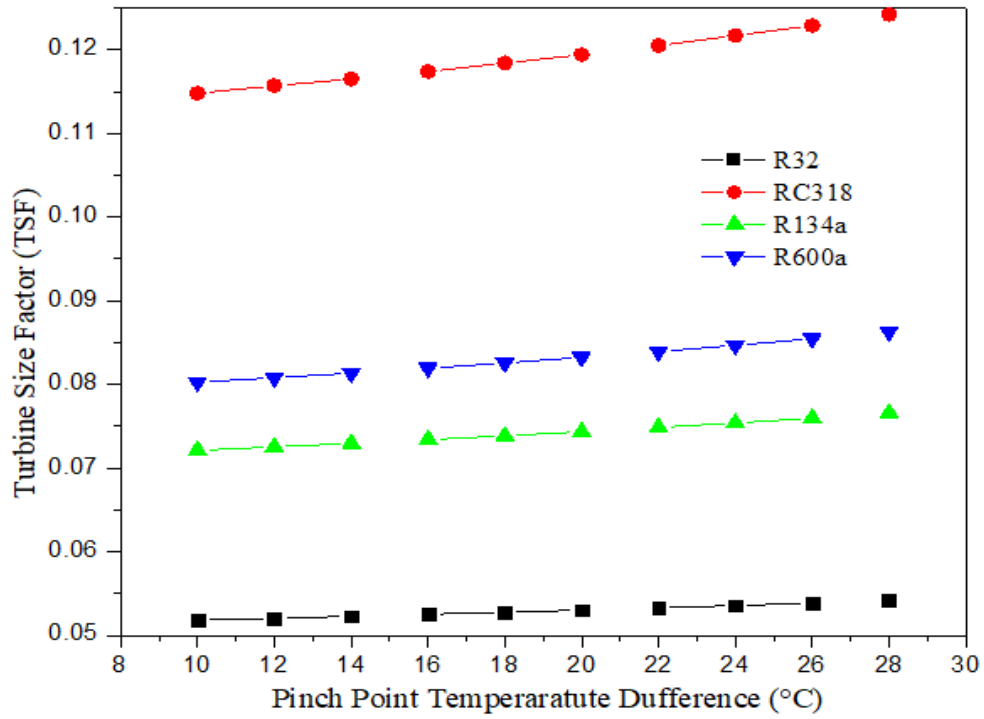


Figure 4.11 Pinch point temperature difference vs. turbine size factor variation

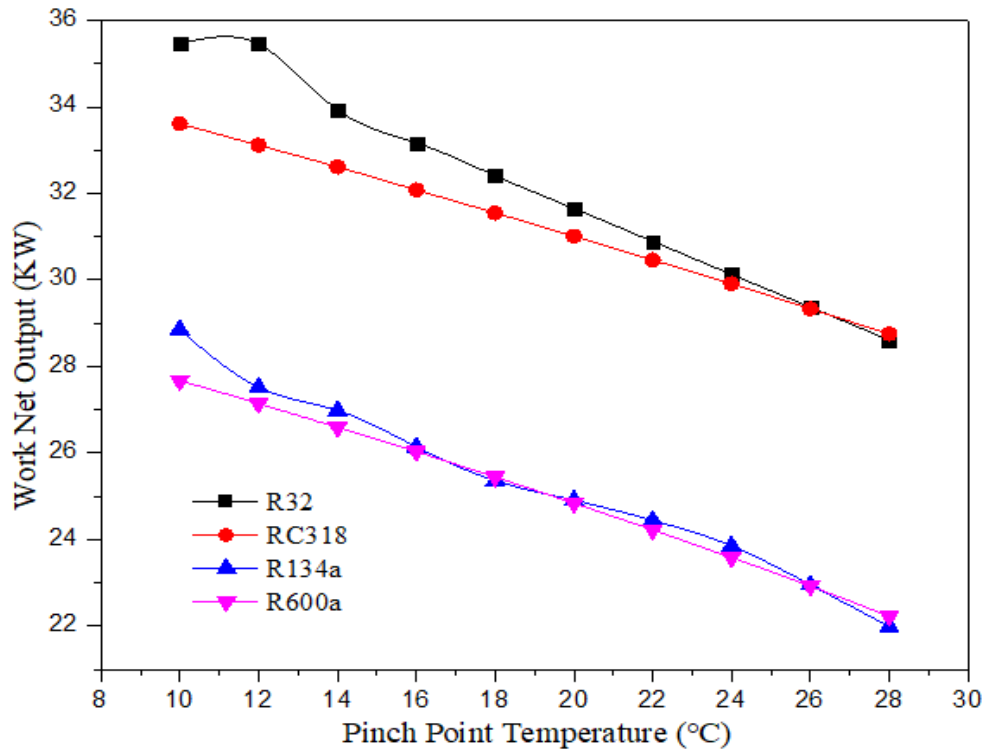


Fig.4.12. Net Work Output Vs. PPTD

4.4 EFFECT OF TURBINE EFFICIENCY

Ist law, IInd law efficiency, TSF and Network output of ORC is analyzed employing R32, R600a, R134a, and RC318 as operating fluid in parametric way. An EES program was developed to analyze the thermodynamic performance parameters as considered by us for the study for various working fluids under varying values of turbine efficiency.

Table 4.13: Simulation results after variation in turbine efficiency using R32

The screenshot shows a window titled 'Parametric Table' with a tab labeled 'Table 4'. The table contains 10 rows of simulation results. The columns are: a run indicator (1..10), turbine efficiency (η_t), first law efficiency (η_I), second law efficiency (η_{II}), and TSF. The values for η_t range from 0.7 to 0.88, η_I from 26.61 to 33.45, η_{II} from 33.61 to 42.26, and TSF from 0.05183 to 0.04662.

1..10	1 η_t	2 η_I	3 η_{II}	4 TSF
Run 1	0.7	26.61	33.61	0.05183
Run 2	0.72	27.37	34.57	0.05121
Run 3	0.74	28.13	35.53	0.0506
Run 4	0.76	28.89	36.49	0.05
Run 5	0.78	29.65	37.45	0.04941
Run 6	0.8	30.41	38.41	0.04884
Run 7	0.82	31.17	39.37	0.04827
Run 8	0.84	31.93	40.34	0.04771
Run 9	0.86	32.69	41.3	0.04716
Run 10	0.88	33.45	42.26	0.04662

Table 4.14: Simulation results after variation in turbine efficiency using R600a

Run	η_t	η_l	η_{ll}	TSF
Run 1	0.7	21.04	26.58	0.1148
Run 2	0.72	21.65	27.34	0.1137
Run 3	0.74	22.25	28.1	0.1125
Run 4	0.76	22.85	28.86	0.1114
Run 5	0.78	23.45	29.62	0.1104
Run 6	0.8	24.05	30.38	0.1093
Run 7	0.82	24.65	31.14	0.1083
Run 8	0.84	25.25	31.9	0.1073
Run 9	0.86	25.85	32.66	0.1063
Run 10	0.88	26.46	33.42	0.1053

Table 4.15: Simulation results after variation in turbine efficiency using R134a

Run	η_t	η_l	η_{ll}	TSF
Run 1	0.7	21.01	26.54	0.07211
Run 2	0.72	21.61	27.3	0.07134
Run 3	0.74	22.21	28.06	0.07059
Run 4	0.76	22.81	28.82	0.06985
Run 5	0.78	23.41	29.58	0.06913
Run 6	0.8	24.02	30.34	0.06843
Run 7	0.82	24.62	31.09	0.06773
Run 8	0.84	25.22	31.85	0.06706
Run 9	0.86	25.82	32.61	0.06639
Run 10	0.88	26.42	33.37	0.06573

Table 4.16: Simulation results after variation in turbine efficiency using RC318

Parametric Table				
Table 1	Table 2	Table 3	Table 4	
1..10	η_t	η_I	η_{II}	TSF
Run 1	0.7	26.67	33.69	0.08026
Run 2	0.72	27.43	34.65	0.07945
Run 3	0.74	28.19	35.61	0.07866
Run 4	0.76	28.96	36.58	0.07788
Run 5	0.78	29.72	37.54	0.07713
Run 6	0.8	30.48	38.5	0.07639
Run 7	0.82	31.24	39.46	0.07567
Run 8	0.84	32	40.43	0.07496
Run 9	0.86	32.77	41.39	0.07427
Run 10	0.88	33.53	42.35	0.07359

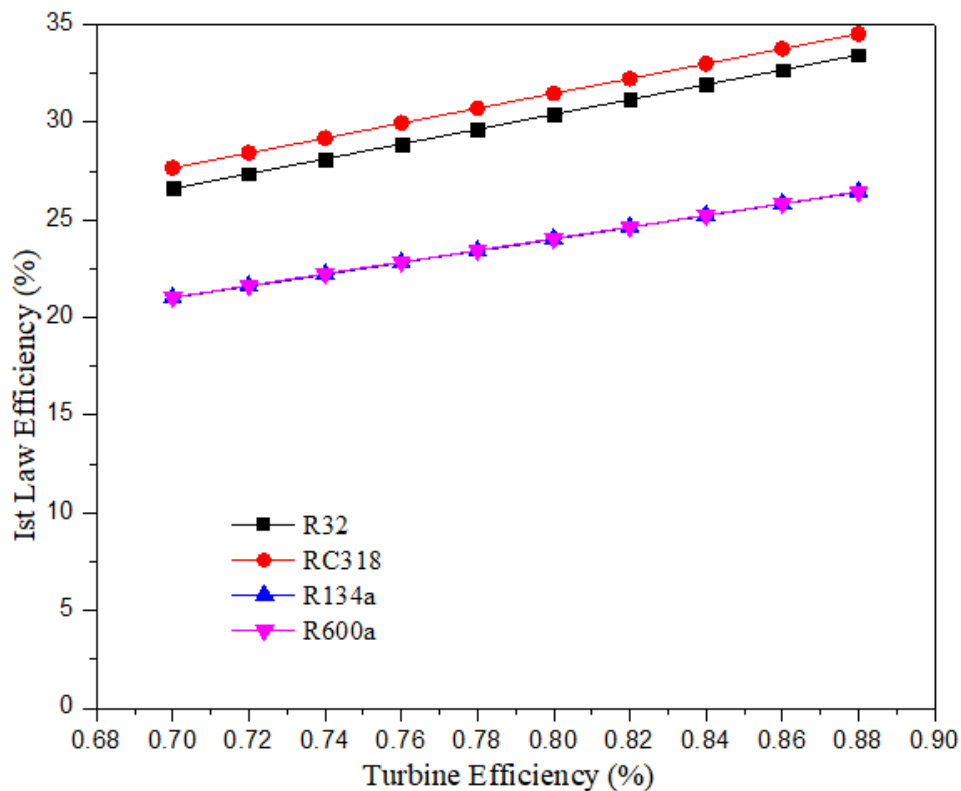


Figure 4.13. Ist law efficiency Vs. TE

By employing different WFs we can observe influence of above parameter. Figure 4.13. depicts Ist law efficiency as function of TE. The effects of turbine efficiency on first law efficiency are found to be consistent across different working fluids. It demonstrates, Ist law thermal efficiency rises in lockstep with TE. In range of 70% to 88% turbine efficiencies with a step of 2%, the Ist law efficiency increases approximately for all the four WFs in consideration. Both RC318 and R32 outperforms R134a and R600a combined in terms of thermal efficiency.

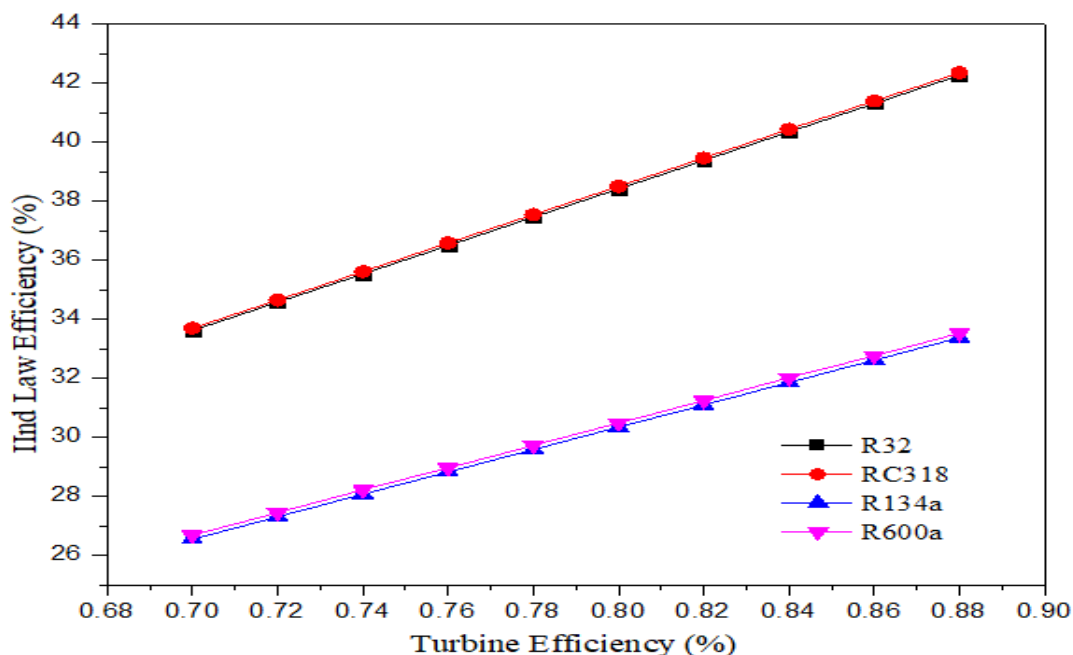


Figure 4.14 IInd law efficiency vs. TE

Influence of turbine efficiency on the ORC's second law efficiency is illustrated in Fig. 4.14. Effects of turbine efficiency on second law efficiency are found to be same when using different operating fluids. It demonstrates that when turbine efficiency rises, the second law thermal efficiency rises in a monotonic fashion. As turbine efficiency rises from 70 percent to 80 percent the IInd law efficiency for all WFs increases monotonically. The best thermal efficiency is obtained by R32 and RC318. R134a and R600a perform poorly.

This is because with increasing TE the actual turbine work increases which in terms increases the Net Work output which is nothing but the difference of turbine work and the pump work. So, with increasing TE, increasing values of Net Work Outputs can be seen for all the Wfs. Here, the Net Work Output increase while the heat supplied remains constant. So, the overall thermal efficiency of the ORC increases with increasing TE.

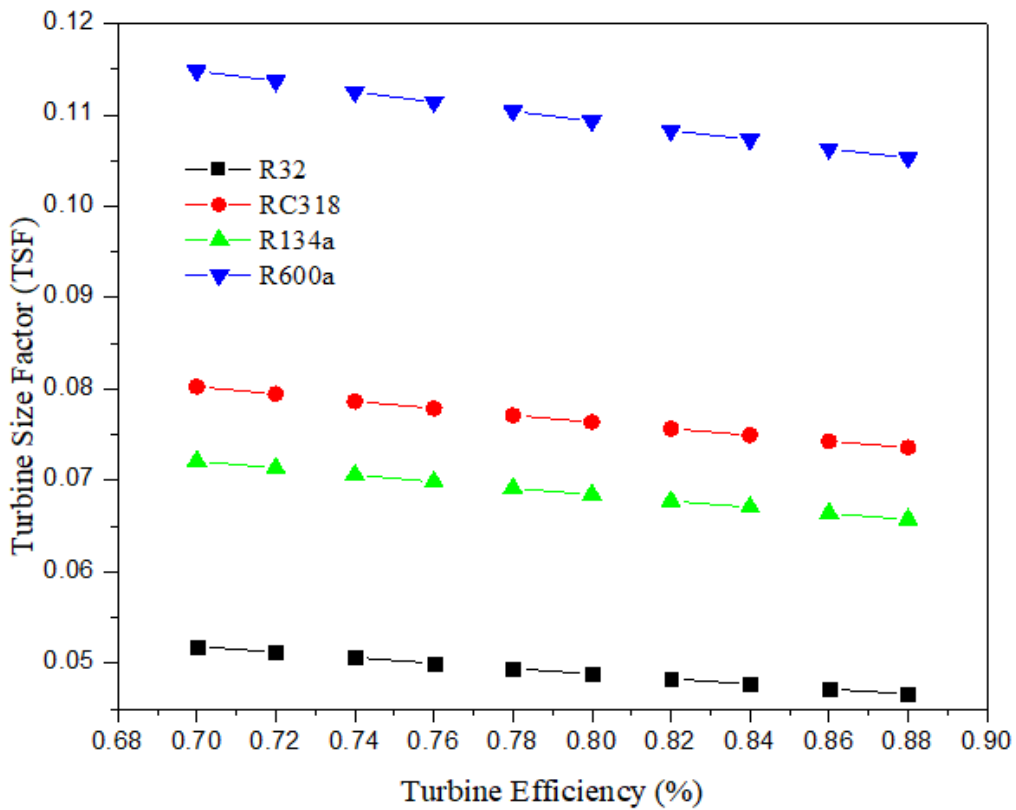


Figure 4.15 TE vs TSF

Figure 4.15 depicts TSF as a function of Turbine efficiency. As the turbine Efficiency rises, TSF falls. Small size factor is achieved for higher turbine efficiency. As a result of low evaporation pressure, R600a requirements greatest size parameter. At all turbine efficiencies, R32 reflects the smallest TSF.

The declining trend of TSF is because of the fact that with increasing TE the volumetric flow rate of refrigerant needed to produce same amount of Net Work Output decreases which reflects towards necessity of a smaller size turbine and hence a lower TSF value can be seen.

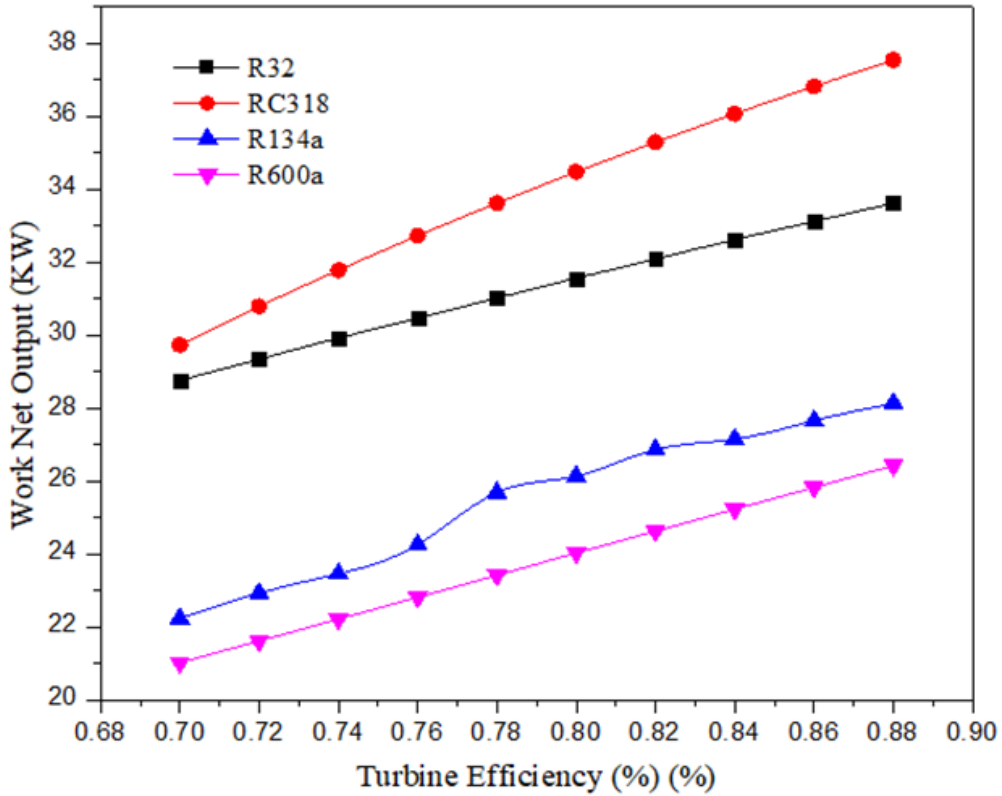


Fig. 4.16 Net Work Output vs. TE

Figure.4.16. depicts Net Work Output as function of Turbine efficiency. It can be inferred that with increase in Turbine efficiency from 70 % to 88% with a step of 2%, Net Work Output increases gradually. Monotonic increase in Net Work outputs can be seen over the range of Turbine efficiency. RC318 reflects highest Net Work Output value over the range of Turbine efficiency while R600a has the lowest one. R32 performs better than R134a, both being wet fluids.

This is because with increasing TE the actual turbine work increases which in terms increases the Net Work output which is nothing but the difference of turbine work and the pump work. So, with increasing TE, increasing values of Net Work Outputs can be seen for all the W

5.1 CONCLUSION

Thermodynamic efficiencies, Net Work Output and TSF of ORC employing R32, R600a, R134a, and RC318 as operating fluid are analyzed and compared. A simulation program in EES has is being designed to determine thermodynamic performance of 4 different operational fluids with different TIT, PPTD, heat source, and turbine efficiency under constant external conditions.

- It is discovered in the current investigation that the effects of heat source temperature on Ist law and IInd law efficiency were equivalent for all those working fluids used. With varying temperature of the source in the range of 100 - 145 °C with step of 5⁰, the Ist and IInd law efficiencies increases approximately considering all the WFs.
- TSF decreases with increase in Temperature of heat source. At high TITs, R32 shows small size factors. Because of the low evaporation pressure, R600a requires the biggest size parameter. Considering the range of TITs, R32 shows the minimum TSP.
- The effect of TIT on the Ist law and IInd law efficiencies were found to be analogous while taking all the four working fluids into consideration. It reveals that when TIT rises, the first law and second law efficiencies increase monotonically. Ist and IInd law efficiencies for R32, R600a, R134a, and RC318 increase precisely as TIT varies from 100 to 370°C. RC318 outperforms R32, R600a and R134a in terms of thermal efficiency.
- When the TIT is increased, the turbine size factor always drops. R32 has small size factors at high TITs for the conditions under consideration. Because of the low evaporation pressure, R600a requires the biggest size parameter. R32 has smallest TSF considering all TITs in the range 100 to 370⁰ with step increase of 30⁰.

- The turbine size factor is always increasing when the TIT is increased. R32 has small size factors at high TITs for the conditions under consideration. Because of the low evaporation pressure, R600a requires the biggest size parameter. R32 realizes the smallest TSP considering all the WFs.
- Effects of turbine efficiency on Ist and IInd law efficiencies were found to be alike while using WFs. It demonstrates that Ist law thermal efficiency rises unvaryingly as turbine efficiency increases. R32 and RC318 realize the best thermal efficiency while R134a and R600a realize lesser thermal efficiency.
- For increasing TIT, the TSF always drops. R32 has small size factors at high TITs for the conditions under consideration. Because of the low evaporation pressure, R600a requires the biggest size parameter. Trifluoroethane (R134a) has the smallest TSP across all TIT.
- For the HST range of 100 to 145^oC the Net Work Output increases gradually. For this case R32 has the highest Net Work output over all the temperature range of heat source followed by RC318, R600a and R134a. R134a shows the least Net Work Output over all the temperature ranges. But the increase is not so significant
- Net Work Output increases for all the four WFs. R32 achieves highest Net Work Output over the range of TITs while RC318, R600a, R134a trailing behind it. R134a has the minimum Net Work Output over all the range of Turbine Inlet Temperature.
- Monotonic increase in Net Work outputs can be seen over the range of Turbine efficiency. RC318 reflects highest Net Work Output value over the range of Turbine efficiency while R600a has the lowest one. R32 performs better than R134a, both being wet fluids.

5.2 FUTURE SCOPE

This research will be continued to look at the impact of superheat as well as the internal heat exchanger (IHx) on thermo-economic performance of the ORC. The working fluids characteristics and heat source are used to compare energy efficiency, net power output.

Effects of working fluid composition ratios and pressure drops in heat exchangers on performance of an ORC system will also be investigated. We'll also improve an ORC recovery system that uses five different waste heat sources.

Abbreviations

ORC	Organic Rankine Cycle
RC	Rankine Cycle
TIT	Turbine inlet Temperature
HST	Heat Source Temperature
TSF	Turbine Size Factor
TSP	Turbine Size Parameter
TE	Turbine Efficiency
VCC	Vapor Compression Cycle
PPTD	Pinch Point Temperature Difference
h	Enthalpy (kJ/KgK)
W_{turbine}	Turbine Work
W_{pump}	Pump work
η_I	I st law efficiency
η_{II}	II nd law efficiency
ΔH	Isentropic Enthalpy difference

References

- [1] Jain, P.K., Arora, A., Arora, B.B. “Performance Analysis of ORC with Environment-Friendly Working Fluids Novec and R1233 as Alternative to R245fa”. *Advances in Energy and Built Environment*. 2020 pages 55-67.
- [2] B. Fankam Tchanche, G. Papadakis, G. Lambrinos, A. Frangoudakis, Fluid selection for a low-temperature solar organic Rankine cycle, *Appl. Therm. Eng.* (2008), <https://doi.org/10.1016/j.applthermaleng.2008.12.025>.
- [3] F. Vélez, J.J. Segovia, M.C. Martín, G. Antolín, F. Chejne, A. Quijano, A technical, economical and market review of organic Rankine cycles for the conversion of low-grade heat for power generation, *Renew. Sustain. Energy Rev.* 16 (2012) 4175–4189, <https://doi.org/10.1016/J.RSER.2012.03.022>.
- [4] J. Larjola, Electricity from industrial waste heat using high-speed organic Rankine cycle (ORC), *Int. J. Prod. Econ.* 41 (1995) 227–235, [https://doi.org/10.1016/0925-5273\(94\)00098-0](https://doi.org/10.1016/0925-5273(94)00098-0).
- [5] D. Wei, X. Lu, Z. Lu, J. Gu, Performance analysis and optimization of organic Rankine cycle (ORC) for waste heat recovery, *Energy Convers. Manag.* (2006), <https://doi.org/10.1016/j.enconman.2006.10.020>.
- [6] Y. Dai, J. Wang, L. Gao, Parametric optimization and comparative study of organic Rankine cycle (ORC) for low grade waste heat recovery, *Energy Convers. Manag.* 50 (2008) 576–582, <https://doi.org/10.1016/j.enconman.2008.10.018>.
- [7] F. Heberle, M. Preißinger, D. Brüggemann, Zeotropic mixtures as working fluids in organic Rankine cycles for low-enthalpy geothermal resources, *Renew. Energy* 37 (2012) 364–370, <https://doi.org/10.1016/J.RENENE.2011.06.044>.
- [8] M. Chys, M. van den Broek, B. Vanslambrouck, M. De Paepe, Potential of zeotropic mixtures as working fluids in organic Rankine cycles, *Energy* 44 (2012) 623–

632<https://doi.org/10.1016/J.ENERGY.2012.05.030>.

[9] T. Deethayat, T. Kiatsiriroat, C. Thawonngamyingsakul, Performance analysis of an organic Rankine cycle with internal heat exchanger having zeotropic working fluid, *Case Stud. Therm. Eng.* 6 (2015) 155–161, <https://doi.org/10.1016/J.CSITE.2015.09.003>.

[10] [S.K. Kalla¹, B.B. Arora, J.A. Usmani “Alternative Refrigerants For HCFC 22—A Review” *Journal of Thermal Engineering*, Vol. 4, No. 3, pp. 1998-2017, April, 2018](#)

[11] J. Bao, L. Zhao, A review of working fluid and expander selections for organic Rankine cycle, *Renew. Sustain. Energy Rev.* 24 (2013) 325–342, <https://doi.org/10.1016/j.rser.2013.03.040>.

[12] N. Chaiyat, T. Kiatsiriroat, Analysis of combined cooling heating and power generation from organic Rankine cycle and absorption system, *Energy* 91 (2015) 363–370, <https://doi.org/10.1016/J.ENERGY.2015.08.057>.

[13] S.H. Kang, Design and experimental study of ORC (organic Rankine cycle) and radial turbine using R245fa working fluid, *Energy* 41 (2012) 514–524, <https://doi.org/10.1016/J.ENERGY.2012.02.035>.

[14] R. Kong, A. Asanakham, T. Deethayat, T. Kiatsiriroat, Heat transfer characteristics of deionized water-based graphene nanofluids in helical coiled heat exchanger for waste heat recovery of combustion stack gas, *Heat. Mass Transf.* (2018) 1–12, <https://doi.org/10.1007/s00231-018-2421-4>.

[15] [S.K. Kalla, B.B. Arora, J.A. Usmani “Performance Analysis of R22 and Its Substitutes in Air Conditioners” *Journal of Thermal Engineering*, Vol. 4, No. 1, pp. 1724-1736, January, 2018](#)

[16] R. Moradi, M. Villarini, E. Habib, E. Bocci, A. Colantoni, L. Cioccolanti, Impact of the expander lubricant oil on the performance of the plate heat exchangers and the scroll expander in a micro-scale organic rankine cycle system, *Appl. Therm. Eng.* 189 (January) (2021),

<https://doi.org/10.1016/j.applthermaleng.2021.116714>

[17] H. Jouhara, N. Khordehgah, S. Almahmoud, B. Delpech, A. Chauhan, S.A. Tassou, Waste heat recovery technologies and applications, *Therm. Sci. Eng. Prog.* 6 (January) (2018) 268–289, <https://doi.org/10.1016/j.tsep.2018.04.017>.

[18] I. Costiuc, L. Costiuc, S. Radu, Waste heat recovery using direct thermodynamic cycle, *Bull. Transilv. Univ. Brasov, Ser. I Eng. Sci.* 8 (2) (2015) 1–6.

[19] A. Nemati, H. Nami, F. Ranjbar, M. Yari, Case studies in thermal engineering a comparative thermodynamic analysis of ORC and Kalina cycles for waste heat recovery: a case study for CGAM cogeneration system, *Case Stud. Therm. Eng.* 2017 (9) (2016) 1–13, <https://doi.org/10.1016/j.csite.2016.11.003>.

[20] T. Tartière, M. Astolfi, A World overview of the organic rankine cycle market the overview the organic rankine assessing the feasibility of the heat, *Energy Procedia* 129 (2017) 2–9, <https://doi.org/10.1016/j.egypro.2017.09.159>.

[21] Y.A. Cengel, M.A. Boles, *Thermodynamics An Engineering Approach*, 8th ed., McGraw-Hill Education, New York, 2015.

[22] I.E. Caceres, R. Agromayor, L.O. Nord, Thermodynamic Optimization of an Organic Rankine Cycle for Power Generation from a Low Temperature Geothermal Heat Source. *Proc. 58th SIMS Sept. 25th - 27th, Reykjavik, Icel. 2011*, 251–262. 10.3384/ecp17138251.

[23] I. Johnson, W.T. Choate, A. Davidson, *Waste Heat Recovery: Technology and Opportunities in U.S. Industry*; BCS Inc., Laurel, MD: United State, 2008. 10.2172/1218716.

[24] C. Campana, L. Cioccolanti, M. Renzi, F. Caresana, Experimental analysis of a small-scale scroll expander for low-temperature waste heat recovery in organic rankine cycle, *Energy* 187 (2019) 115929, <https://doi.org/10.1016/j.energy.2019.115929>.

[25] C. Spadacini, L.G. Xodo, M. Quaia, Geothermal energy exploitation with organic rankine cycle technologies, in: *Organic Rankine Cycle (ORC) Power Systems*, Elsevier Ltd, Italy, 2017,

pp. 473–525. 10.1016/B978-0-08-100510-1.00014-4.

[26] A.D. Pasek, T.A.F. Soelaiman, C. Gunawan, Thermodynamics study of flashbinary cycle in geothermal power plant, *Renew. Sustain. Energy Rev.* 15 (9) (2011) 5218–5223, <https://doi.org/10.1016/j.rser.2011.05.019>.

[27] DiPippo, R. Binary Cycle Power Plants. In *Geothermal Power Plant Principles, Applications, Case Studies and Environmental Impact*; Massachusetts, 2016; pp 193–239. 10.1016/B978-0-08-100879-9.00008-2.

[28] S. Clemente, D. Micheli, M. Reini, R. Taccani, Energy efficiency analysis of organic Rankine cycles with scroll expanders for cogenerative applications, *Appl. Energy* 97 (2012) 792–801, <https://doi.org/10.1016/j.apenergy.2012.01.029>.

[29] J. Zhu, Z. Chen, H. Huang, Y. Yan, Effect of resistive load on the performance of an organic Rankine cycle with a scroll expander, *Energy* 95 (2016) 21–28, <https://doi.org/10.1016/j.energy.2015.11.048>.

[30] M. Lukawski, Design and optimization of standardized organic Rankine cycle power plant for European conditions, *RES: The School for Renewable Energy Science: Akuyreyri*, 2009

[31] G. Bamorovat Abadi, E. Yun, K.C. Kim, Experimental study of a 1 Kw organic rankine cycle with a zeotropic mixture of R245fa/R134a, *Energy* 93 (2015) 2363–2373, <https://doi.org/10.1016/j.energy.2015.10.092>.

[32] I. National Refrigerant, National Refrigerant Reference Guide, 6th ed., National Refrigerant Inc, Philadelphia, 2016.

[33] S.P. Dutta, R.C. Borah, Design of a solar organic Rankine cycle prototype for 1 KW power output, *Int. J. Eng. Trends Technol.* 62 (1) (2018) 23–33.

[34] R. Moradi, M. Villarini, L. Cioccolanti, Experimental modeling of a lubricated, open drive scroll expander for micro-scale organic Rankine cycle systems, *Appl. Therm. Eng.* 190 (February) (2021), <https://doi.org/10.1016/j.applthermaleng.2021.116784> 116784.

- [34] M. Imran, M. Usman, B. Park, D. Lee, Volumetric expanders for low grade heat and waste heat recovery applications, *Renew. Sustain. Energy Rev.* 57 (2016) 1090–1109, <https://doi.org/10.1016/j.rser.2015.12.139>.
- [36] O. Dumont, R. Dickes, V. Lemort, Experimental investigation of four volumetric expanders, *Energy Procedia* 129 (2017) 859–866, <https://doi.org/10.1016/j.egypro.2017.09.206>.
- [37] F. Alshammari, M. Usman, A. Pesyridis, Expanders for Organic Rankine Cycle Technology, *IntehcOpen*, 2018, pp. 41–59, <https://doi.org/10.5772/intechopen.78720>. [24] National Refrigerant, I. Technical Guidelines R-134a; Philadelphia, 2010.
- [38] H. Xi, M. Li, H. Zhang, Y. He, Experimental studies of organic Rankine cycle systems using scroll expanders with different suction volumes, *J. Clean. Prod.* 218 (2019) 241–249, <https://doi.org/10.1016/j.jclepro.2019.01.302>.
- [39] N. Zhou, X. Wang, Z. Chen, Z. Wang, Experimental study on organic Rankine cycle for waste heat recovery from low-temperature Fl Ue gas, *Energy* 55 (2013) 216–225, <https://doi.org/10.1016/j.energy.2013.03.047>.
- [40] Virang H Oza, Nilesh M Bhatt, Optimization of Ammonia-Water Absorption Refrigeration System using Taguchi Method of Design of Experiment, *International Journal of Mechanics and Solids*, 13(2), 111-126, 2018.
- [41] K. S. AlQdah, “Performance and evaluation of aqua ammonia auto air conditioner system using exhaust waste energy”, *Energy Procedia*, vol. 6, 2011.
- [42] Satish Raghuvanshi, Govind Maheshwari, Analysis of Ammonia –Water (NH₃-H₂O) Vapor Absorption Refrigeration System based on First Law of Thermodynamics, *International Journal of Scientific & Engineering Research*, 2(8), 1-7, 2011.
- [43] Manzela, S. M. Hanriot, L. C. Gomez, and J. R. Sodre, “Using engine exhaust gas as an energy source for an absorption refrigeration system”, *Applied Energy*, vol. 87, 2010.

[44] Aman Shukla, C.O.P Derivation and Thermodynamic Calculation of Ammonia-Water

[45] Vapor Absorption Refrigeration System, International Journal of Mechanical Engineering and Technology, 6(5), 72-81, 2015.

[46] Yadav and B. R. Singh, “Experimental set up of air conditioning system in automobile using exhaust energy”, S-jpset, vol. 5, 2014.

[47] Ahmed Ouadha, Youcef El-Gotni (2013), Integration of an ammonia-water absorption refrigeration system with a marine Diesel engine: A thermodynamic study, The 3rd International Conference on Sustainable Energy Information Technology, Procedia Computer Science, 19, 754 – 761.

[48] C. V. Vazhappilly, T. Tharayil, A.P. Nagarajan, “Modeling and experimental analysis of generator in vapor absorption refrigeration system”, Journal of Engineering Research and Application, vol. 3, no. 5, 2013.

[49] Ehsan Akrami, Hossein Nami, , Faramarz, Ranjbar, “Hydrogen production using the waste heat of Benchmark pressurized Molten carbonate fuel cell system via combination of organic Rankine cycle and proton exchange membrane (PEM) electrolysis’ Applied Thermal Engineering, Volume 114, 5 March 2017, Pages 631-638

[50] Sotirios Karellas and Konstantinos Braimakis “Energy–exergy analysis and economic investigation of a cogeneration and tri-generation ORC–VCC hybrid system utilizing biomass fuel and solar power’ Energy Conversion and Management, Volume 107, 1 January 2016, Pages 103-113

[51] M.Jradi and S.Riffat Experimental investigation of a biomass-fuelled micro-scale tri-generation system with an organic Rankine cycle and liquid desiccant cooling unit’ Energy, Volume 71, 15 July 2014, Pages 80-93

[52] Riccardo Amirante ,Sergio Bruno, Elia Distaso, Massimo L, Scalab PaoloTamburrano. ‘A biomass small-scale externally fired combined cycle plant for heat and power generation in rural communities’ Renewable Energy Focus, Volume 28, March 2019, Pages 36-46

[53] Hadi Rostanzadeh and Pejman Nouranib “Investigating potential benefits of a salinity gradient solar pond for ejector refrigeration cycle coupled with a thermoelectric generator” Energy, Volume 172, 1 April 2019, Pages 675-690

[54] Huawei Chang, Zhongmin Wana Yao Zhenga Xi Chen, Shuiming Shu , Zhengkai TucdSiew ,Hw Chand “Energy analysis of a hybrid PEMFC–solar energy residential micro-CCHP system combined with an organic Rankine cycle and vapor compression cycle” Energy Conversion and Management, Volume 142, 15 June 2017, Pages 374-384

[57]Shyam Agarwal, Akhilesh Arora, B.B.Arora “ Energy and exergy analysis of vapor compression–triple effect absorption cascade refrigeration system” Engineering Science and Technology, an International Journal Volume 23, Issue 3, June 2020, Pages 625-641

[58] Neeraj Kumar, BB Arora, S Maji, “Influence of Alternative Fuels on Exhaust Emissions of IC Engine: A Review” Renewable Energy Optimization, Planning and Control. 2022, Pages 11-29

[59] Subrata Kumar Patra, Tilak Raj, BB Arora. “An analysis and modelling of selected barriers for a sustainable manufacturing system using ISM technique” International Journal of Operational Research. Volume 41, Issue 3, June 2021, Pages 373-398.

[60] Hardial Singh, BB Arora. Effects of casing angle on the performance of parallel hub axial annular diffuser” International Journal of Turbo & Jet-Engines. 2020.

List Of Publications

- [1] S. S. Rout and B. B. Arora, "Effect of Working Fluids in Thermodynamic Performance Analysis of Organic Rankine Cycle (ORC)", *International Journal of Mechanical Engineering*, Vol. 7, No. 5, pp. 1054-1067, May, 2022.

Available: https://kalaharijournals.com/resources/MAY_126.pdf